European Journal of Medicinal Chemistry 132 (2017) 26–41

Contents lists available at ScienceDirect

European Journal of Medicinal Chemistry

journal homepage: http://www.elsevier.com/locate/ejmech

Research paper

Discovery of 2-substituted 1*H*-benzo[*d*]immidazole-4-carboxamide derivatives as novel poly(ADP-ribose)polymerase-1 inhibitors with in vivo anti-tumor activity

Jie Zhou [a, 1], Ming Ji [b, 1], Zhixiang Zhu [b], Ran Cao [a], Xiaoguang Chen [b, **], Bailing Xu [a, *]

[a] Beijing Key Laboratory of Active Substance Discovery and Druggability Evaluation, Institute of Materia Medica, Chinese Academy of Medical Sciences & Peking Union Medical College, Beijing, 100050, China
[b] State Key Laboratory of Bioactive Substances and Functions of Natural Medicines, Institute of Materia Medica, Chinese Academy of Medical Sciences & Peking Union Medical College, Beijing, 100050, China

ARTICLE INFO

Article history:
Received 3 January 2017
Received in revised form
6 March 2017
Accepted 8 March 2017
Available online 18 March 2017

Keywords:
PARP-1 inhibitor
PARP-2 inhibitor
Benzo[*d*]immidazole-4-carboxamide
Anti-tumor agents

ABSTRACT

Novel 1*H*-benzo[*d*]immidazole-4-carboxamide derivatives bearing five-membered or six-membered *N*-heterocyclic moieties at the 2-position were designed and synthesized as PARP-1 inhibitors. Structure-activity relationships were conducted and led to a number of potent PARP-1 inhibitors having IC_{50} values in the single or double digit nanomolar level. Some potent PARP-1 inhibitors also had similar inhibitory activities against PARP-2. Among all the synthesized compounds, compound **10a** and **11e** displayed strong potentiation effects on temozolomide (TMZ) in MX-1 cells (PF_{50} = 7.10, PF_{50} = 4.17). In vivo tumor growth inhibition was investigated using compound **10a** in combination with TMZ, and it was demonstrated that compound **10a** could strongly potentiate the cytotoxicity of TMZ in MX-1 xenograft tumor model. Two co-crystal structures of compounds **11b** and **15e** complexed with PARP-1 were achieved and demonstrated a unique binding mode of these benzo-imidazole derivatives.

1. Introduction

Poly (ADP-ribose) polymerase-1 (PARP-1) is an abundant nuclear enzyme, discovered five decades ago, and is involved in the repair process of DNA damage [1,2]. As a molecular sensor of DNA strand breaks, PARP-1 can detect the DNA damage and bind to the nicks through its N-terminal domain, and its catalytic domain on C-terminal can locate the nicotinamide adenine dinucleotide (NAD^+) as substrate and catalyze the conversion of NAD^+ into nicotinamide and ADP-ribose units. The ADP-ribose units were transferred to proteins participating in the repair pathway including histone and PARP-1 itself and formed ADP-ribose polymers on the substrate proteins. This post-transcriptional poly-ADP-ribosylation has a pivotal role in the repair of DNA damage, in particular for the single strand breaks repair through base excursion repair pathway [3–7]. It has been suggested that PARP-1 was strongly activated in tumor cells when DNA damaging agents were used as anti-cancer therapeutics, and resulted in drug resistance. Therefore, inhibiting PARP-1 could potentiate the toxicity of chemotherapeutics such as temozolomide (TMZ) and cisplatin in the combination therapy [8–12]. Even more interestingly, it was found that PARP-1 was synthetic lethal with BRCA1/2, which is involved in DNA double strand breaks repair through homologous recombination pathway. This synthetic lethality conferred tumor cells with BRCA1/2 mutations more susceptible to PARP-1 inhibitors, which could be used as a single agent in the treatment of BRCA defective cancers [13–16]. In fact, PARP-1 inhibitors were mainly exploited as a treatment modality for patients with BRCA dysfunctions in clinical trials for the present.

As targeting the repair pathway of DNA damage has been recognizing as an intriguing manoeuvre for coping with cancers, PARP-1 inhibitors have aroused a great deal of interests among academics and pharmaceutical industries. A significant number of structurally diversified PARP-1 inhibitors were developed and a dozen of inhibitors have been advanced into clinical trials, including ABT-888, AZD2281, AG014699, MK-4827 and BMN673 [17–23]. Among them, Olaparib (AZD-2281) was the first PARP-1 inhibitor approved by FDA in 2014 for the treatment of high-

* Corresponding author.
** Corresponding author.
E-mail addresses: chxg@imm.ac.cn (X. Chen), xubl@imm.ac.cn (B. Xu).
[1] The first two authors contributed equally.

http://dx.doi.org/10.1016/j.ejmech.2017.03.013
0223-5234/

grade serous ovarian cancer. Although tremendous progress has been made in researches on PARP-1 inhibitors, it is still an exciting and imperative for the development of novel chemical entities with varied pharmacodynamic and pharmacokinetic properties, so as to PARP-1 inhibitors would be able to become effective treatments for multiple cancers.

The substrate NAD^+ binds in the catalytic domain of PARP-1 and the binding region was usually characterized as two sub-pockets. One is the nicotinamide-ribose binding site (NI site) and the other is the adenine-ribose binding site (AD site). The known PARP-1 inhibitors take full advantage of the NI site through hydrogen bonds with residues Ser904 and Gly863, and π-π stacking interaction with Tyr907. In comparison with NI site, the AD site has more space to accommodate diverse structural motifs, and some of known PARP-1 inhibitors including AZD-2281 utilized this pocket to improve their potency and PK properties [24,25]. In this work, we took benzo[*d*]immidazole-4-carboxamide as a core structure to occupy the NI site since it was successfully employed in potent PARP-1 inhibitors such as ABT-888, and NU1085 [17,26]. Furthermore, various substituted cyclic amines were tentatively selected and introduced on the 2-position of benzo[*d*]imidazole ring to explore additional bindings within AD site. Herein, we described the chemical synthesis and biological evaluation of the designed 2-subsituted benzo[*d*]imidazole derivatives as PARP-1 inhibitors. The biological evaluations were performed with respect to enzymatic inhibition, potentiation effects on DNA damaging agent and antitumor activity in MX-1 xenograft tumor model. Two co-crystal structures were also presented to elicit the action mode of the designed molecules.

2. Chemical synthesis

The 1*H*-benzo[*d*]immidazole-4-carboxamide derivatives were prepared according to the synthetic route as outlined in Scheme 1 and their chemical structures were presented in Tables 1–4. Upon treatment with methyl 2,2,2-trichloroacetimidate and TFA, 2,3-diamino-benzamides (**1** and **2**) were converted into 2-(trichloromethyl)-1*H*-benzo[*d*]imidazole-4-carboxamides (**3** and **4**) in 61% and 92% yields, respectively. Under the basic reaction conditions, compounds **3** and **4** were hydrolyzed into the corresponding carboxylic acids **5** and **6** in high yields, which were the key intermediates for preparation of various designed target molecules. Compounds **5** and **6** were coupled with 1-substituted pyrrolidin-3-amine, 1-substituted piperidin-3-amine or 1-substituted piperidin-4-amine generating series of compounds **7**–**10** (Tables 1 and 2) in moderate to good yields. And compounds **5** and **6** were subjected to condensation reaction with *N*-Boc pyrrolidin-3-amine or *N*-Boc piperidin-4-amine, followed by Boc deprotection, reductive amination or acylation giving rise to series of compounds **11**–**14** (Table 3) in reasonable yields. Regarding series of compounds **15** and **16** (Table 4) bearing piperazine, hydropyrrolo[3,4-*b*]pyridine, or quinuclidin-3-amine motif, they were readily prepared by condensation of compounds **5** and **6** with the corresponding amines followed by Boc deprotection or acylation reaction.

3. Results and discussion

3.1. Enzymatic activity against PARP-1

The inhibitory activities against PARP-1 of all target compounds (**7a-7c, 8a-8f, 9a-9o, 10a, 10b, 11a-11g, 12a-12c, 13a-13e, 14a-14c, 15a-15k, 16a, 16b**) were evaluated. ABT888 and AZD2281 were used as reference molecules. The corresponding results were expressed as IC_{50} values and presented in Tables 1–4

Initially, 3-amino-pyrrolidine and 3-amino-piperidine derivatives (**7a-7c, 8a-8f**) were prepared and their inhibitory activities were shown in Table 1. Generally, these compounds moderately inhibited PARP-1 enzymatic activity and had IC_{50} values ranging from 199 nM to 1810 nM. And in both series compounds, introduction of bulky substituents on the nitrogen would lead to decrease in potency, when compared with non-substituted compounds **7c** and **8e**.

We also synthesized 4-amino-piperidine derivatives (**9a-9o** and **10a-10b** in Table 2) in order to probe the impact of the nitrogen position in the piperidine ring on the inhibitory activity. Compound **9a** with a Boc group showed moderate inhibitory activity against PARP-1 with an IC_{50} value of 644 nM, while removal of the Boc (compound **9o**) resulted in 6-fold enhancement on potency, suggesting that the Boc is somewhat larger for this position. Satisfyingly, it was found that incorporation of a small to mediate size alkyl group on the piperidine ring (compounds **9b-9g**) produced marked inhibition effect on PARP-1 with IC_{50} values in the double digit nanomolar level. In contrast, when a bulkier substituent was placed on the nitrogen, compounds **9j-9n** exhibited decreased activity. It was demonstrated that larger moieties with carbon atoms $\geq$5 were not tolerated on the nitrogen, while smaller hydrophobic groups would be beneficial for the binding affinity. Notably, compound **9i** with a *neo*-pentyl group on the nitrogen had IC_{50} value of 41 nM and it was more potent than isomers **9j** and **9k**, presumably because the shape of *neo*-pentyl substituent was well matched with that of the sub-pocket.

Compounds **10a** and **10b** with a fluoro atom on the 6-position of benzo-imidazole ring were highly active against PARP-1 (IC_{50}: 17 nM and 30 nM), and their inhibition was stronger than that of corresponding non-fluoro-substituted counterparts (compounds **9i** and **9k**), respectively. It was demonstrated that grafting a fluoro atom on the 6-position would be favorable for the binding affinity, and this result was consistent with the known SARs. Additionally, in comparison with 3-amino-piperidine derivatives, 4-amino-piperidine moiety seems to be a proper choice for generating potent PARP-1 inhibitors, since compounds **9a** and **9o** are somewhat more active than compounds **8a** and **8e**.

When 3-amino-pyrrolidine and 4-amino-piperidine fragments were linked to the benzo-imidazole scaffold through the ring nitrogen atom resulted in series of compounds **11**–**14** (Table 3). These compounds showed a wide range of inhibitory activities against PARP-1 with IC_{50} values varying from 2.76 nM to 1190 nM. In general, a bulky group, such as Boc or *N*-Boc-piperidine-4-yl substituent taken as the R group would deteriorate the potency, as exemplified by compounds **11a**, **11f**, **13a** and **13d**. Removal of the Boc group had a significant positive impact on the inhibition and led to the potency increasing more than 10-fold (**11a** *vs* **11b, 12a** *vs* **12b, 13a** *vs* **13b, 14a** *vs* **14b**), suggesting a basic amine group was desirable in this position, presumably a strong hydrogen bond or electrostatic interaction formed between the amine group and an acidic residue within the PARP-1 catalytic site. Moreover, compounds (**11c-11e, 12c, 13c, 14c**) with an alkyl hydrophobic group, such as a propyl or cyclohexyl moiety on the nitrogen had comparable potency with non-substituted derivatives, demonstrating that variations on the nitrogen by hydrophobic groups were allowed and this provided an opportunity for improving structural diversity and physicochemical properties. Compared with 3-amino-pyrrolidine derivatives (**11b** *vs* **12b, 11e** *vs* **12c**), grafting a fluoro atom on the 6-position had a more favorable effect on the inhibition in 4-amino-piperidine derivatives (**13b** *vs* **14b, 13c** *vs* **14c**). In fact, compounds **14b** (IC_{50} = 2.76 nM) and **14c** (IC_{50} = 7.54 nM) are the most potent PARP-1 inhibitors in this series of benzo-imidazole derivatives, they had single digit nanomolar activities.

We also incorporated the piperazine, piperazin-2-one and other

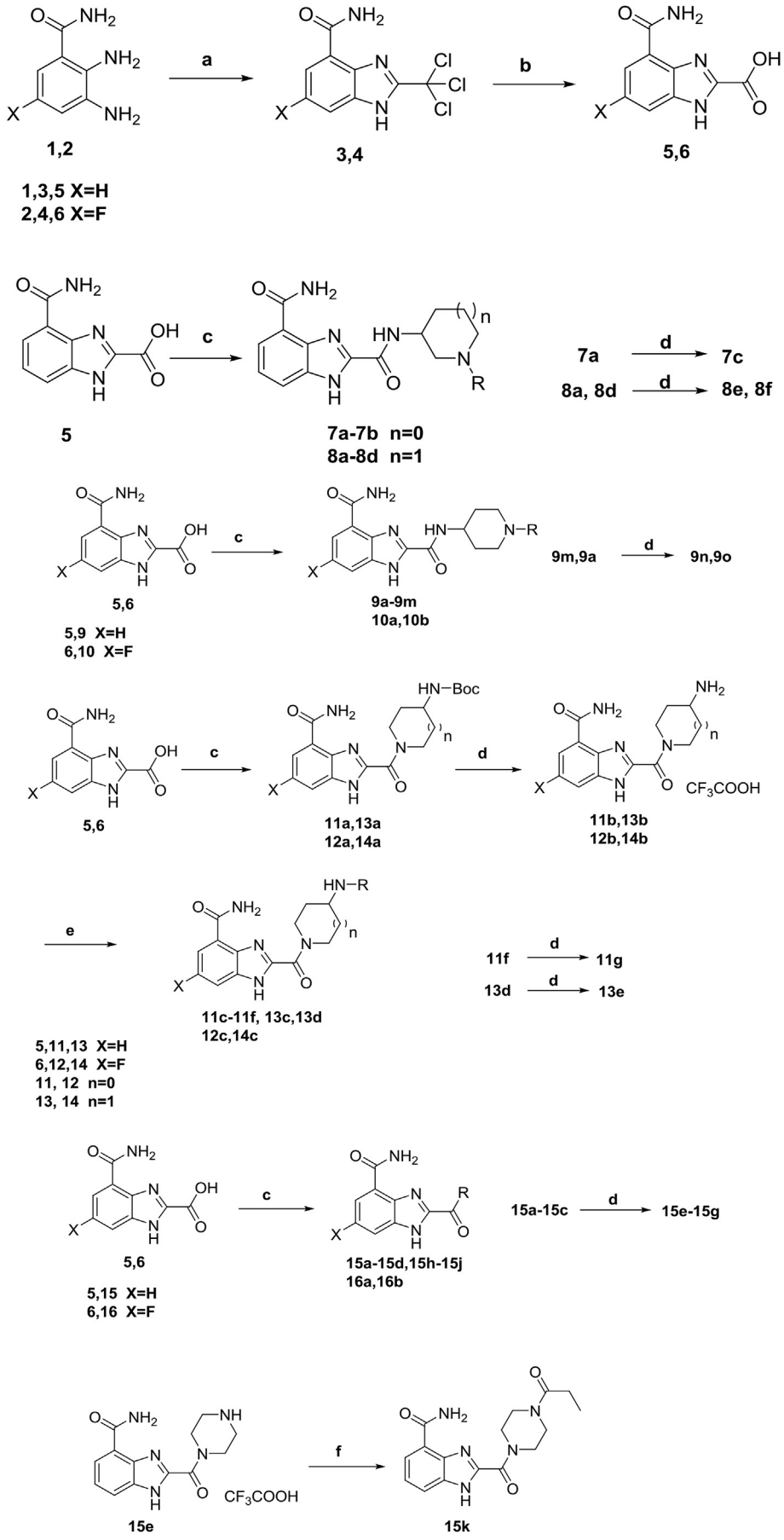

Scheme 1. Reagents and conditions: a) methyl 2,2,2-trichloroacetimidate, TFA, DCM, ether, rt; b) NaOH (aq, 1 N), H_2O, rt; c) EDC, HOBt, Et_3N, DMF, rt or HBTU, HOBt, DIEA, DMF, rt; d) TFA, DCM, rt; e) acyl chloride, DCM, Et_3N, or aldehyde or ketone, DIEA, THF, then $NaBH(OAc)_3$; (f) propionyl chloride, DCM, Et_3N, 0 °C.

bulky *N*-heterocyclic fragments into the 2-position of benzo-imidazole core to further expand the SARs. As shown in Table 4, similar to previous derivatives (Tables 1–3), Boc derivatives had low potency in comparison with non-substituted compounds (**15a** *vs* **15e, 15b** *vs* **15f**). Regarding piperazine series, alkylation on the nitrogen with *iso*-butyl group (compound **15d**, $IC_{50} = 81$ nM) was tolerated, while acylation with propionyl moiety (compound **15k**, $IC_{50} > 100$ nM) produced reduced activity, indicating that a basic amine group was necessary for the binding, probably functioning as an H-bond donor or an acceptor. In addition, comparing compound **15f** bearing an ethyl group on the piperizine ring with **15g**, the (*S*)-enantiomer (**15f,** $IC_{50} = 19$ nM) was >5 times more potent than the (*R*)-enantiomer (**15g,** $IC_{50} > 100$ nM). Thus we considered compound **15f** was deserved to be further optimized in terms of its structural novelty and potent enzymatic activity. As to the piperazin-2-one derivatives (**15j, 16a** and **16b**), these compounds displayed strong inhibition effect on PARP-1, suggesting that piperazin-2-one could be exploited as an alternative motif for achieving potent PARP-1 inhibitors. In addition, compounds **15h** and **15i** showed low inhibitory activity and their IC_{50} values of >100 nM. Therefore, bulky heterocyclic amines were not preferred as the structural motifs to be incorporated into the 2-position of benzo-imidazole scaffold.

3.2. Enzymatic activity against PARP-2 and cellular potency

PARP-2 is the closest homolog of PARP-1 in the PARP superfamily and its catalytic domain shares 69% similarity to that of PARP-1. Furthermore, both enzymes are involved in DNA breaks repair and PARP-1 contributes >90% PARP activity [27]. It has been well known that most of PARP-1 inhibitors were also recognized as PARP-2 inhibitors with comparable potency, although these inhibitors were initially designed to target PARP-1. In this work, we selected some potent PARP-1 inhibitors to test their inhibition effects on PARP-2. As shown in Table 5, these benzo-imidazole derivatives presented somewhat stronger inhibition on PARP-1 over PARP-2, and none of them showed selectivity more than 10 fold though.

The cellular potency of twelve PARP-1 inhibitors was evaluated by measuring their potentiation effects on TMZ-induced cytotoxicity in MX-1 cells. As presented in Table 5, among the tested derivatives, compounds **10a** and **11e** could strongly sensitize the cytotoxicity of TMZ in MX-1 breast cancer cells. The cytotoxicity of TMZ was increased to 7.1 fold and 4.17 fold, respectively, when TMZ was used in combination with 10 μM concentration of compounds **10a** and **11e**. Of note, some compounds had remarkable enzymatic potency, however, they could not potentiate the cytotoxicity of TMZ in MX-1 cells, e.g. compounds **12b**, **14b** and **14c**, presumably due to the poor permeability. Therefore, it is worthwhile to note that improving both PARP-1 inhibitory activity and cellular potency could be achieved by variations of the R group on the benzo-imidazole ring.

3.3. In vivo antitumor activity of compound *10a*

As compound **10a** showed remarkable potentiation effects on TMZ-induced cytotoxicity in MX-1 cells, we further tested its anti-cancer activity as a sensitizer of TMZ using MX-1 xenograft tumor model. The results were outlined in Table 6. Orally dosing TMZ (50 mg/kg) to the BalB/c nude mice bearing MX-1 xenograft tumors obviously resulted in tumor growth inhibition in 62%, while compound **10a** was administered at a dose of 50 mg/kg did not inhibit the tumor growth. However, when compound **10a** were used with TMZ in combination, both dosing at 50 mg/kg, the tumors shrunk markedly and 88% tumor growth inhibition was achieved. When TMZ treated group was used as the control, the combination dosing still produced 68% inhibition effect. It was demonstrated that compound **10a** was a strong chemo-sensitizing agent. Additionally, it was observed that the combination treatment did not lead to pronounced body weight changes, suggesting that compound **10a** had low toxicity at this dose.

4. Crystal structures of compounds 11b and 15e complexed with PARP-1

The co-crystal structures of compounds **11b** and **15e** located in the catalytic site of PARP-1 were obtained with an aim to investigate the binding features of the designed benzo-imidazole-based PARP-1 inhibitors. As shown in Fig. 1, as we expected, the benzo-imidazole scaffold was nicely situated in NI site and formed 3 key hydrogen bonds with the backbone of Gly863 and the side chain of Ser904. It also formed characterized π–π stacking with Tyr907. These binding features were consistent with that of the known PARP-1 inhibitors [4,28]. The 3-amino-pyrrolindine ring extended into AD site, and especially the amino group interacted with Asp766 via a favorable charge-charge interaction, which was considered to have great positive contributions to the binding affinity of this series of PARP-1 inhibitors. In fact, this indeed gave a good explanation for previous SAR. Removal of the Boc group resulted in dramatic enhancement in potency.

As shown in Fig. 2, the binding mode of compound **15e** was the same as that of compound **11b**. In this co-crystal structure, the nitrogen on the piperazine ring formed the key charge-charge interaction with Asp766. It has been reported that Asp766 could be exploited to construct novel PARP-1 inhibitors. However, few known PARP-1 inhibitors presented this interaction in their binding, except for ABT-888 [29]. Therefore, this unique binding interaction in this class of PARP-1 inhibitors deserved to be further explored, and it might provide a chance to build up more potent PARP-1 inhibitors with distinct binding features by modifications on the amine group.

5. Conclusion

In summary, novel 2-substituted benzo[*d*]imidazole-4-carboxamide derivatives were designed based on the characteristics of the catalytic domain in PARP-1. The enzymatic inhibition results demonstrated that incorporation of a 3-aminopyrrolidine fragment on the 2-position via the ring nitrogen can give rise to potent PARP-1 inhibitors with IC_{50} values in the double digit nanomolar level (compounds **11b** and **12b**). The co-crystal structure of **11b** located in PARP-1 proved that the basic 3-amino group on the pyrrolidine ring was critical for the binding since it created a key electrostatic interaction with Asp766. More importantly, various six-membered *N*-heterocyclic moieties, such as 4-amino piperidine, piperizine, (S)-2-ethyl piperizine and piperizin-2-one were allowed to be integrated into the 2-position of benzo-imidazole scaffold. These derivatives produced strong inhibitory effects on PARP-1, and the most potent inhibitors (**14b** and **14c**) had IC_{50} value of single digit nanomolar level. These diversified structure motifs provided numerous opportunities to further develop potent PARP-1 inhibitors with unique structure properties and physiochemical properties. Furthermore, compound **10a** demonstrated high efficacy as a sensitizer of TMZ in MX-1 xenograft tumor model, suggesting that these benzo-imidazole-based PARP-1 inhibitors could be developed into useful anti-tumor agents.

Table 1
The chemical structures and PARP-1 inhibitory activities of compounds **7a-7c**, **8a-8f**[a].

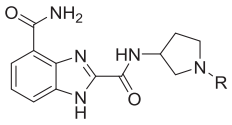

7a-7c

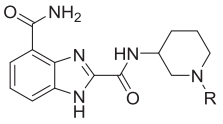

8a-8f

Compd.	R	PARP-1 IC_{50}[b](nM) ±SD[c]	Compd.	R	PARP-1 IC_{50}[b](nM) ±SD[c]
7a	Boc	1810 ± 152	**8c**	cyclohexyl	382 ± 8
7b	cyclohexyl	>1000	**8d**	*N*-Boc-piperidine-4-yl	818 ± 75
7c	H	343 ± 14	**8e**	H	199 ± 24
8a	Boc	1150 ± 87	**8f**	piperdine-4-yl	793 ± 37
8b	*iso*-pentyl	708 ± 10			

[a] The ability of compounds to inhibit PARP-1 enzyme activity were tested using NAD^+ method and ABT888 was used as a positive control. The measured IC_{50} for ABT-888 was132 nM.
[b] Concentrations for 50% inhibition in PARP-1 enzyme assay (IC_{50}).
[c] Standard Deviation.

Table 2
The chemical structures and PARP-1 inhibitory activities of compounds **9a-9o**, **10a-10b**[a].

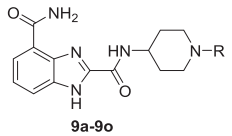

9a-9o

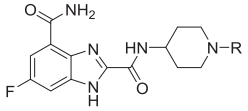

10a-10b

Compd.	R	PARP-1 IC_{50}[b](nM) ±SD[c]	Compd.	R	PARP-1 IC_{50}[b](nM) ±SD[c]
9a	Boc	644 ± 21	**9j**	*iso*-pentyl	111 ± 7
9b	ethyl	40 ± 5	**9k**	pentan-3-yl	302 ± 12
9c	trifluoroethyl	34 ± 4	**9l**	cyclohexyl	311 ± 24
9d	trifluoroacetyl	83 ± 7	**9m**	*N*-Boc-piperidine-4-yl	868 ± 45
9e	propyl	49 ± 5	**9n**	piperidine-4-yl	316 ± 23
9f	*iso*-propyl	64 ± 4	**9o**	H	101 ± 11
9g	*iso*-butyl	92 ± 8	**10a**	*neo*-pentyl	17 ± 3
9h	cyclopropylmethyl	108 ± 11	**10b**	pentan-3-yl	30 ± 5
9i	*neo*-pentyl	41 ± 5			

[a] The ability of compounds to inhibit PARP-1 enzyme activity were tested using ELISA method and ABT888 or AZD2281 was used as a positive control. The measured IC_{50} for ABT-888 was 5.18 nM, and IC_{50} for AZD-2281 was 2.09 nM.
[b] Concentrations for 50% inhibition in PARP-1 enzyme assay (IC_{50}).
[c] Standard Deviation.

6. Experimental section

6.1. Chemical synthesis general

Unless otherwise noted, all materials were obtained from commercial suppliers and used without further purification. All reactions involving air- or moisture-sensitive reagents were performed under an argon atmosphere. Melting points were measured on a Yanaco micro melting point apparatus and are uncorrected. 1H NMR (300 MHz and 400 MHz) on a Varian Mercury spectrometer was recorded in DMSO-d_6 or $CDCl_3$. Chemical shifts are reported in δ (ppm) units relative to the internal standard tetramethylsilane (TMS). High resolution mass spectra (HRMS) were obtained on an Agilent Technologies LC/MSD TOF spectrometer. All chemicals and solvents used were of reagent grade without purified or dried before use. All the reactions were monitored by thin-layer chromatography (TLC) on pre-coated silica gel G plates at 254 nm under a UV lamp. Column chromatography separations were performed with silica gel (200–300 mesh).

Table 3
The chemical structures and PARP-1 inhibitory activities of compounds **11a-11g, 12a-12c, 13a-13e, 14a-14c**[a].

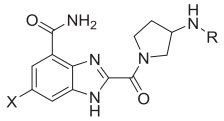

11a-11g, 12a-12c

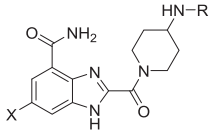

13a-13e, 14a-14c

Compd.	X	R	PARP-1 IC_{50}[b](nM) ±SD[c]	Compd.	X	R	PARP-1 IC_{50}[b](nM) ±SD[c]
11a	H	Boc	857 ± 99	**12c**	F	cyclohexyl	37 ± 3
11b	H	H	15 ± 3	**13a**	H	Boc	968 ± 45
11c	H	propyl	79 ± 8	**13b**	H	H	29 ± 3
11d	H	propionyl	83 ± 6	**13c**	H	cyclohexyl	70 ± 6
11e	H	cyclohexyl	75 ± 7	**13d**	H	*N*-Boc-piperidine-4-yl	250 ± 27
11f	H	*N*-Boc-piperidine-4-yl	1190 ± 68	**13e**	H	piperidine-4-yl	316 ± 13
11g	H	piperidine-4-yl	60 ± 5	**14a**	F	Boc	80 ± 14
12a	F	Boc	>100	**14b**	F	H	2.76 ± 0.47
12b	F	H	12 ± 3.46	**14c**	F	cyclohexyl	7.54 ± 0.85

[a] The ability of compounds to inhibit PARP-1 enzyme activity were tested using ELISA method and ABT888 or AZD2281 was used as a positive control. IC_{50} for ABT-888 was 5.18 nM and for AZD-2281 was 2.09 nM.
[b] Concentrations for 50% inhibition in PARP-1 enzyme assay (IC_{50}).
[c] Standard Deviation.

6.2. Synthesis of compounds

6.2.1. tert-Butyl 3-(4-carbamoyl-1H-benzo[d]imidazole-2-carboxamido)pyrrolidine-1-carboxylate (**7a**)

A mixture of 2-carboxyl-1*H*-benzo[*d*]immidazole-4-carboxamide (75 mg, 0.37 mmol), EDC (210 mg, 1.09 mmol), HOBt (147 mg, 1.09 mmol), Et_3N (0.4 mL, 2.93 mmol) and *N*-Boc-aminopyrrolidine (202 mg, 1.09 mmol) in DMF (5 mL) was stirred at room temperature for 20 h and then H_2O was added to the mixture. The solution was extracted with the solvent mixture (ethyl acetate/methanol = 10:1) (30 mL × 3) and then the organic layer was washed with brine (20 mL × 2). The combined organic layer was dried over anhydrous $MgSO_4$. After filtration and concentration, the crude product was obtained and purified with column chromatography (methylene chloride/methanol = 50:1 to 40:1) to give compound **7a** as a white solid (74 mg, 54.4%); mp 231–233 °C; Compound **7a** exists as a mixture of two conformers; ^{1}H NMR (300 MHz, DMSO-d_6) δ (ppm): 13.68 (s, 1H), 9.27 (d, J = 7.2 Hz, 1H), 9.16 (brs, 1H), 7.93 (d, J = 7.5 Hz, 1H), 7.83 (brs, 1H), 7.70 (d, J = 8.1 Hz, 1H), 7.42 (t, J = 7.5 Hz, 1H), 4.50–4.60 (m, 1H), 3.55–3.65 (m, 1H), 3.38–3.47 (m, 2H), 3.24–3.31 (m,1H), 2.12–2.23 (m, 1H), 1.94–2.08 (m, 1H), 1.40 (s, 9H); ^{13}C NMR (100 MHz, DMSO-d_6) δ (ppm): 165.72, 158.30, 153.48, 145.43, 139.85, 134.89, 123.96, 123.86, 123.56, 116.39, 78.43, 50.14 (49.91), 49.09 (48.42), 44.26 (44.01), 30.83 (30.01), 28.17; HRMS (ESI): *m/z*, calcd. For $C_{18}H_{24}N_5O_4$ $[M+H]^+$ 374.1823, found 374.1812.

This method was used to prepare compounds 7b, 8a-8d, 9a-9m, 11a, 13a, 15a-15d.

6.2.2. N^2-(1-cyclohexylpyrrolidin-3-yl)-1H-benzo[d]imidazole-2,4-dicarboxamide (**7b**)

Compound **7b** was obtained as a white solid (70 mg, 33%); mp 229–232 °C; ^{1}H NMR (300 MHz, DMSO- d_6) δ (ppm): 13.68 (brs, 1H), 9.33 (s, 1H), 9.15 (s, 1H), 7.93 (d, J = 6.9 Hz, 1H), 7.79 (s, 1H), 7.71 (d, J = 7.2 Hz, 1H), 7.42 (t, J = 7.5 Hz, 1H), 4.57 (brs, 1H), 2.80–3.50 (m, 5H), 2.26 (brs, 1H), 1.95 (brs, 2H), 1.72 (brs, 2H), 1.56 (d, J = 9.3 Hz, 1H), 1.16–1.40 (m, 6H); ^{13}C NMR (100 MHz, DMSO- d_6) δ (ppm): 165.60, 158.07, 145.25, 139.98, 134.78, 124.02, 123.94, 116.13, 62.77, 54.85, 49.48, 47.32, 29.62, 28.63, 24.78, 24.10; HRMS (ESI): *m/z*, calcd. For $C_{19}H_{26}N_5O_2$ $[M + H]^+$ 356.2081, found 356.2075.

6.2.3. N^2-(Pyrrolidin-3-yl)-1H-benzo[d]imidazole-2,4-dicarboxamide 2,2,2-trifluoroacetate (**7c**)

To a solution of compound **7a** in DCM (5.0 mL), TFA (0.27 mL, 4.23 mmol) was added and then the reaction mixture was stirred at room temperature for 2 h. Ether (20 mL) was added into the mixture. After filtration, the title compound **7c** was afforded as a white solid (35 mg, 58%); mp 233–235 °C; ^{1}H NMR (300 MHz, DMSO-d_6) δ (ppm): 13.74 (brs, 1H), 9.29 (d, J = 5.7 Hz, 1H), 9.11 (s, 1H), 9.00 (brs, 2H), 7.94 (d, J = 7.5 Hz, 1H), 7.88 (brs, 1H), 7.72 (d, J = 7.5 Hz, 1H), 7.43 (t, J = 7.8 Hz, 1H), 4.55–4.70 (m, 1H), 3.23–3.52 (m, 4H), 2.24–2.29 (m, 1H), 2.09–2.14 (m, 1H); HRMS (ESI): *m/z*, calcd. For $C_{13}H_{16}N_5O_2$ $[M + H]^+$ 274.1299, found 274.1293.

6.2.4. tert-Butyl 3-(4-carbamoyl-1H-benzo[d]imidazole-2-carboxamido)piperidine-1-carboxylate (**8a**)

Compound **8a** was obtained as a white solid (90 mg, 15.9%); mp 226–228 °C; ^{1}H NMR (400 MHz, DMSO-d_6) δ (ppm): 13.70 (s, 1H), 9.15 (s, 1H), 9.04 (d, J = 6.8 Hz, 1H), 7.93 (d, J = 6.8 Hz, 1H), 7.85 (s, 1H), 7.71 (d, J = 7.6 Hz, 1H), 7.43 (t, J = 7.2 Hz, 1H), 4.10 (brs, 1H), 3.80–3.88 (m, 2H), 2.72–2.82 (m, 1H), 1.92–1.98 (m, 1H), 1.68–1.78 (m, 2H), 1.39–1.50 (m, 11H); ^{13}C NMR (100 MHz, DMSO-d_6) δ (ppm): 166.18, 158.23, 154.35, 145.98, 140.27, 135.35, 124.41, 124.28, 123.99, 116.83, 79.30, 47.80, 46.43, 43.65, 30.06, 28.49, 24.34; HRMS (ESI): *m/z*, calcd. For $C_{19}H_{26}N_5O_4$ $[M + H]^+$ 388.1979, found 388.1969.

6.2.5. N^2-(1-iso-Pentylpiperidin-3-yl)-1H-benzo[d]imidazole-2,4-dicarboxamide (**8b**)

Compound **8b** was obtained as a white solid (75 mg, 33.6%); mp

Table 4
The chemical structures and PARP-1 inhibitory activities of compounds **15a-15k, 16a, 16b**[a].

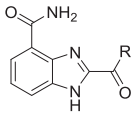

15a-15k

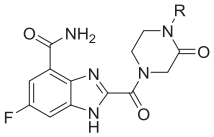

16a,16b

Compd.	R	PARP-1 IC_{50}[b](nM) ±SD[c]	Compd.	R	PARP-1 IC_{50}[b](nM) ±SD[c]
15a	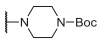	152 ± 11	**15h**		>100
15b	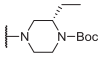	100 ± 13	**15i**		116 ± 10
15c	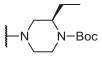	>100	**15j**		29 ± 2
15d	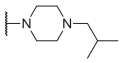	81 ± 7	**15k**	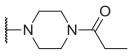	>100
15e		42 ± 3	**16a**	H	15 ± 5
(S)-15f		19 ± 2	**16b**	pentan-3-yl	88 ± 31
(R)-15g		>100			

[a] The ability of compounds to inhibit PARP-1 enzyme activity were tested using ELISA method and ABT888 or AZD2281 was used as a positive control. The measured IC_{50} for ABT-888 was 5.18 nM, IC_{50} for AZD-2281 was 2.09 nM.
[b] Concentrations for 50% inhibition in PARP-1 enzyme assay (IC_{50}).
[c] Standard Deviation.

216–218 °C; ^{1}H NMR (400 MHz, DMSO-d_6) δ (ppm): 13.65 (brs, 1H), 9.12 (s, 1H), 8.91 (d, J = 7.2 Hz, 1H), 7.93 (d, J = 7.2 Hz, 1H), 7.82 (s, 1H), 7.70 (d, J = 7.6 Hz, 1H), 7.41 (t, J = 8.0 Hz, 1H), 3.99 (brs, 1H), 2.86 (brs, 1H), 2.71 (brs, 1H), 2.32 (brs, 2H), 2.03 (brs, 1H), 1.93 (brs, 1H), 1.83 (brs, 1H), 1.68 (brs, 1H), 1.49–1.60 (m, 3H), 1.31–1.33 (m, 2H), 0.86 (d, J = 6.4 Hz, 6H); HRMS (ESI): *m/z*, calcd. For $C_{19}H_{28}N_5O_2$ $[M + H]^+$ 358.2238, found 358.2231.

6.2.6. N^2-(1-cyclohexylpiperidin-3-yl)-1H-benzo[d]imidazole-2,4-dicarboxamide (*8c*)

Compound **8c** was obtained as a white solid (90 mg, 35.8%); mp 247–248 °C; ^{1}H NMR (400 MHz, DMSO-d_6) δ (ppm): 13.65 (brs, 1H), 9.11 (s, 1H), 8.88 (d, J = 6.8 Hz, 1H), 7.93 (d, J = 7.2 Hz, 1H), 7.82 (brs, 1H), 7.70 (d, J = 7.6 Hz, 1H), 7.41 (t, J = 7.6 Hz, 1H), 3.97 (brs, 1H), 2.84 (brs, 1H), 2.69 (brs, 1H), 2.22–2.31 (m, 3H), 1.71–1.80 (m, 6H), 1.48–1.56 (m, 3H), 1.13–1.28 (m, 4H), 0.99–1.08 (m, 1H); ^{13}C NMR (100 MHz, DMSO-d_6) δ (ppm): 165.61, 157.53, 145.50, 140.00, 134.72, 123.94, 123.82, 116.13, 63.69, 52.46, 48.41, 45.53, 29.25, 27.31, 25.40, 25.12; HRMS (ESI): *m/z*, calcd. For $C_{20}H_{28}N_5O_2$ $[M + H]^+$ 370.2238, found 370.2232.

6.2.7. tert-Butyl 3-(4-carbamoyl-1H-benzo[d]imidazole-2-carboxamido)-1,4'-bipiperidine-1'- carboxylate (*8d*)

Compound **8d** was obtained as a white solid (200 mg, 43.6%); mp 238–240 °C; ^{1}H NMR (400 MHz, DMSO-d_6) δ (ppm): 13.65 (s, 1H), 9.12 (s, 1H), 8.90 (d, J = 8.4 Hz, 1H), 7.93 (d, J = 7.6 Hz, 1H), 7.82 (s, 1H), 7.69 (d, J = 8.0 Hz, 1H), 7.41 (t, J = 8.0 Hz, 1H), 3.97 (brs, 3H), 2.86 (d, J = 9.6 Hz, 1H), 2.63–2.72 (m, 3H), 2.45 (brs, 1H), 2.27 (t, J = 9.6 Hz, 1H), 2.19 (brs, 1H), 1.81 (brs, 1H), 1.66–1.69 (m, 3H), 1.48–1.50 (m, 2H), 1.37 (s, 9H), 1.27–1.31 (m, 2H); ^{13}C NMR (100 MHz, DMSO-d_6) δ (ppm): 165.59, 157.53, 153.67, 145.47, 140.02, 134.70, 123.96, 123.87, 123.71, 116.14, 78.71, 61.73, 48.38, 42.57, 28.03, 26.96; HRMS (ESI): *m/z*, calcd. For $C_{24}H_{35}N_6O_4$ $[M + H]^+$ 471.2714, found 471.2708.

6.2.8. N^2-(Piperidin-3-yl)-1H-benzo[d]imidazole-2,4-dicarboxamide 2,2,2-trifluoroacetate (*8e*)

The title compound was synthesized from **8a** using the same method as the preparation of compound **7c**: Compound **8e** was obtained as a white solid (48 mg, 71.6%); mp 156–158 °C; ^{1}H NMR (400 MHz, DMSO-d_6) δ (ppm): 13.72 (brs, 1H), 9.18 (d, J = 8.0 Hz, 1H), 9.08 (brs, 1H), 8.88 (brs, 1H), 8.72 (brs, 1H), 7.94 (d, J = 7.6 Hz, 1H), 7.87 (s, 1H), 7.72 (d, J = 8.0 Hz, 1H), 7.43 (d, J = 8.0 Hz, 1H), 4.25 (brs, 1H), 3.37–3.39 (m, 1H), 3.26 (d, J = 11.6 Hz, 1H), 2.94 (q, J = 10.4 Hz, 1H), 2.75–2.89 (m, 1H), 1.90–1.96 (m, 2H), 1.68–1.74 (m, 2H); ^{13}C NMR (100 MHz, DMSO-d_6) δ (ppm): 165.69, 157.84, 145.24, 139.66, 135.14, 124.02, 123.92, 123.49, 116.52, 45.90, 43.38, 42.91, 28.07, 20.78; HRMS (ESI): *m/z*, calcd. For $C_{14}H_{18}N_5O_2$ $[M + H]^+$ 288.1455, found 288.1451.

Table 5
The enzymatic activities against PARP-1 and PARP-2 and potentiation effects on TMZ in MX-1 cells of selected compounds.

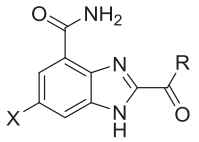

Compd	X	R	PARP-1 IC_{50}[a](nM) ±SD[c]	PARP-2 IC_{50}[a](nM) ±SD[c]	PF_{50}[b]
9c	H	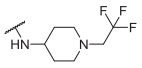	34 ± 4	100 ± 9	0.93
9h	H	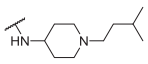	108 ± 11	130 ± 9	3.53
9o	H	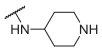	101 ± 11	ND	1.75
10a	F	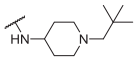	17 ± 3	74 ± 6	7.10
11b	H	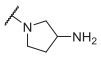	15 ± 3	48 ± 3	1.98
11c	H	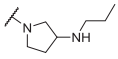	79 ± 8	75 ± 5	1.54
11e	H	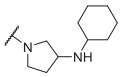	75 ± 7	91 ± 2	4.17
12b	F	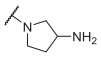	12 ± 3.46	19 ± 1	1.07
12c	F	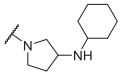	37 ± 3	38 ± 4	1.71
13b	H	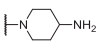	29 ± 3	73 ± 3	1.99
14b	F	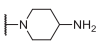	2.76 ± 0.47	24 ± 2	0.98
14c	F	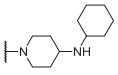	7.54 ± 0.85	34 ± 3	0.71

[a] The ability of compounds to inhibit PARP-1 and PARP-2 enzyme activity were tested using ELISA method and AZD2281 was used as a positive control. The measured IC_{50} against PARP-1 was 2.09 nM, the measured IC_{50} against PARP-2 was 2.26 nM.
[b] Potentiation factor (PF_{50}): The fold of potentiation was calculated as the ratio of the IC_{50} for TMZ divided by the IC_{50} of TMZ + PARP-1 inhibitor, the test compounds were used at a fixed concentration of 10 μM.
[c] Standard Deviation.

Table 6
In vivo tumor growth inhibition of compound **10a.**

Group	Number start/end	Tumor weights(g±SE)	$\%T/C_{veh}$(%TGI)	Weight change(g)	$\%T/C_{TMZ}$(%TGI)
Vehicle	6/6	4.09 ± 0.64	NA	5.32	NA
TMZ(50 mg/kg)	6/6	1.57 ± 0.64	38 (62)***	0.02	NA
TMZ+10a (25 mg/kg)	6/6	1.47 ± 0.68	36 (64)***	0.23	94(6)
TMZ+10a (50 mg/kg)	6/6	0.50 ± 0.10	12 (88)***	−0.79	32(68)
10a (50 mg/kg)	6/6	3.73 ± 0.64	91 (9)	5	NA

NA: Not Applicable, ANOVA, ***$p < 0.001$ vs Vehicle.

*6.2.9. N^2-(1,4′-Bipiperidine-3-yl) 1H-benzo[d]imidazole-2,4-dicarboxmide 2,2,2-trifluoroacetate (**8f**)*

The title compound was synthesized from **8d** using the same method as the preparation of compound **7c**: Compound **8f** was obtained as a white solid (100 mg, 80%); mp 171–173 °C; ^{1}H NMR (400 MHz, DMSO-d_6) δ (ppm): 13.68 (brs, 1H), 10.20 (brs, 1H), 9.26 (brs, 1H), 9.10 (brs, 1H), 8.92 (brs, 1H), 8.61 (brs, 1H), 7.95 (d, J = 7.2 Hz, 1H), 7.88 (s, 1H), 7.71 (d, J = 7.2 Hz, 1H), 7.44 (t, J = 7.6 Hz, 1H), 4.33 (brs, 1H), 3.47 (brs, 7H), 2.92 (brs, 3H), 2.22 (brs, 2H), 2.00 (brs, 2H), 1.60–1.90 (m, 3H); HRMS (ESI): *m/z*, calcd. For $C_{19}H_{27}N_6O_2$ $[M + H]^+$ 371.2190, found 371.2183.

*6.2.10. tert-Butyl 4-(4-carbamoyl-1H-benzo[d]imidazole-2-carboxamido)piperidine-1-carboxylate (**9a**)*

Compound **9a** was obtained as a white solid (130 mg, 46%); mp. 251–253 °C; ^{1}H NMR (300 MHz, DMSO- d_6) δ (ppm): 13.62 (s, 1H),

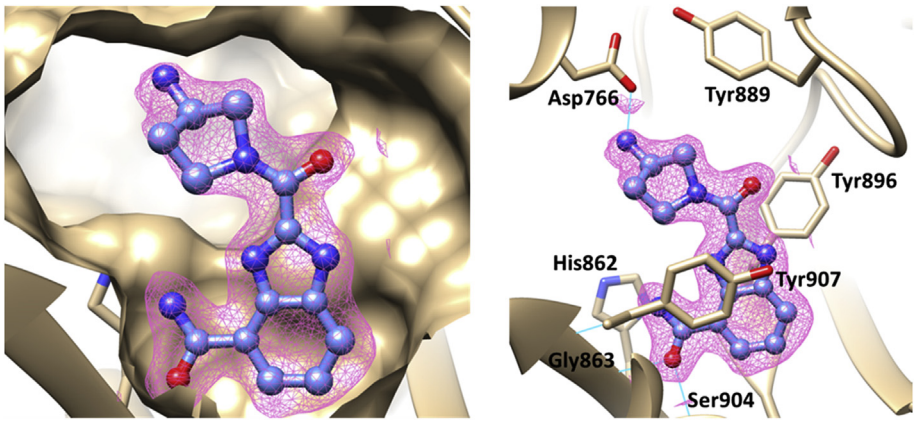

Fig. 1. Co-crystal structure of PARP-1 in complex with **11b**. Protein and ligand structures are colored in tan and sky blue, respectively. Hydrogen bonds are represented with cyan lines. The $2F_o–F_c$ electron density map (contoured at 1σ) around the inhibitor is shown as pink mesh (PDB: 5WS1). (For interpretation of the references to colour in this figure legend, the reader is referred to the web version of this article.)

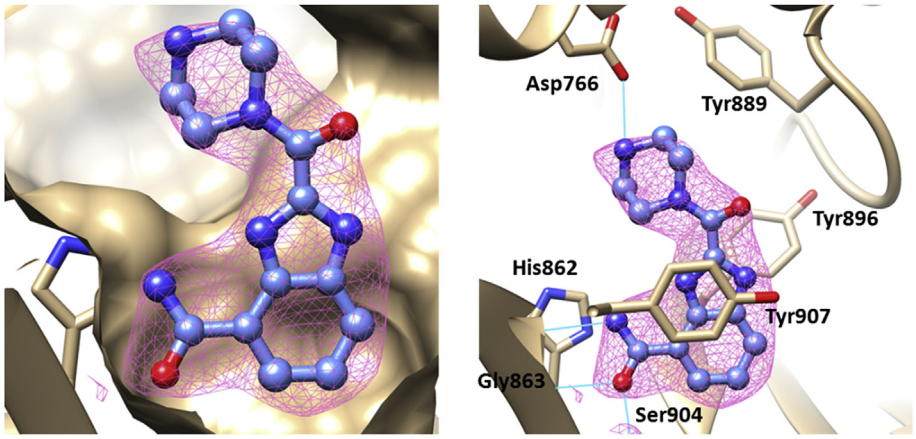

Fig. 2. Co-crystal structure of PARP-1 in complex with 15e. Protein and ligand structures are colored in tan and sky blue, respectively. Hydrogen bonds are represented with cyan lines. The $2F_o–F_c$ electron density map (contoured at 1σ) around the inhibitor is shown as pink mesh (PDB: 5WS0). (For interpretation of the references to colour in this figure legend, the reader is referred to the web version of this article.)

8.81 (s, 1H), 7.92 (d, J = 6.9 Hz, 1H), 7.81 (s, 1H), 7.72 (d, J = 7.8 Hz, 1H), 7.43 (t, J = 8.1 Hz, 1H), 6.94 (d, J = 7.5 Hz, 1H), 4.85 (d, J = 12.3 Hz, 1H), 4.38 (d, J = 12.9 Hz, 1H), 3.61 (brs, 1H), 3.43 (t, J = 12.3 Hz, 1H), 3.05 (t, J = 12.6 Hz, 1H), 1.83 (brs, 2H), 1.38–1.48 (m, 11H); HRMS (ESI): *m/z*, calcd. For $C_{19}H_{25}N_5O_4$ $[M + H]^+$ 388.1979, found 388.1971.

*6.2.11. N^2-(1-Ethylpiperidin-4-yl)-1H-benzo[d]imidazole-2,4-dicarboxamide (**9b**)*

Compound **9b** was obtained as a white solid (70 mg, 30.4%); mp 272–274 °C; ^{1}H NMR (400 MHz, DMSO-d_6) δ (ppm): 13.60 (brs, 1H), 9.14 (brs, 1H), 9.07 (d, J = 8.0 Hz, 1H), 7.92 (d, J = 7.2 Hz, 1H), 7.80 (s, 1H), 7.70 (d, J = 8.0 Hz, 1H), 7.40 (t, J = 7.6 Hz, 1H), 3.85 (brs, 1H), 2.98 (d, J = 10.8 Hz, 2H), 2.42 (q, J = 10.8 Hz, 2H), 2.09 (t, J = 10.8 Hz, 2H), 1.65–1.85 (m, 4H), 1.02 (t, J = 7.2 Hz, 3H); ^{13}C NMR (100 MHz, DMSO-d_6) δ (ppm): 165.71, 157.31, 145.62, 139.93, 134.83, 123.88, 123.76, 116.28, 50.95, 50.72, 45.70, 29.46, 10.36; HRMS (ESI): *m/z*, calcd. For $C_{16}H_{22}N_5O_2$ $[M + H]^+$ 316.1768, found 316.1764.

*6.2.12. N^2-(1-(2,2,2,-Trifluoroethyl) piperidin-4-yl)-1H-benzo[d] imidazole-2,4-dicarboxamide (**9c**)*

Compound **9c** was obtained as a white solid (49 mg, 26.5%); mp 276–278 °C; ^{1}H NMR (400 MHz, DMSO-d_6) δ (ppm): 13.65 (s, 1H), 9.17 (s, 1H), 9.05 (d, J = 7.6 Hz, 1H), 7.95 (d, J = 7.6 Hz, 1H), 7.83 (s, 1H), 7.71 (d, J = 8.0 Hz, 1H), 7.42 (t, J = 8.0 Hz, 1H), 3.87 (brs, 1H), 3.19 (q, J = 10.0 Hz, 2H), 2.98 (d, J = 11.2 Hz, 2H), 2.47 (t, J = 10.4 Hz, 2H), 1.74–1.79 (m, 4H); ^{13}C NMR (400 MHz, DMSO-d_6) δ (ppm): 165.64, 157.42, 145.74, 140.07, 134.67, 126.08 (q, J_{CF} = 278.5), 123.89, 123.76, 123.68, 116.08, 56.67 (q, J_{CF} = 29.0), 52.82, 46.19, 31.18; HRMS (ESI): *m/z*, calcd. For $C_{16}H_{19}N_5O_2F_3$ $[M + H]^+$ 370.1485, found 370.1480.

*6.2.13. N^2-(1-(2,2,2,-Trifluoroacetyl) piperidin-4-yl)-1H-benzo[d] imidazole-2,4-dicarboxamide (**9d**)*

Compound **9d** was obtained as a white solid (50 mg, 17.9%); mp > 300 °C; ^{1}H NMR (400 MHz, DMSO-d_6) δ (ppm): 13.70 (s, 1H), 9.13 (s, 2H), 9.09 (d, J = 8.0 Hz, 1H), 7.92 (d, J = 8.0 Hz, 1H), 7.84 (s, 1H), 7.69 (d, J = 8.0 Hz, 1H), 7.41 (t, J = 8.0 Hz, 1H), 4.36 (d, J = 9.2 Hz, 1H), 4.20–4.29 (m, 1H), 3.92 (d, J = 9.2 Hz, 1H), 3.41 (t, J = 9.2 Hz, 1H), 3.08 (t, J = 9.2 Hz, 1H), 1.99 (t, J = 9.2 Hz, 2H), 1.51–1.52 (m, 2H); ^{13}C NMR (100 MHz, DMSO-d_6) δ (ppm): 165.74, 157.48, 154.09 (q, J_{CF} = 34.6), 145.58, 140.04, 134.77, 123.97, 123.84, 123.60, 116.47 (q, J_{CF} = 286.8), 116.19, 45.71, 44.44, 42.46, 31.68, 30.77; HRMS (ESI): *m/z*, calcd. For $C_{16}H_{17}N_5O_3F_3$ $[M + H]^+$ 384.1278, found 384.1276.

*6.2.14. N^2-(1-Propylpiperidin-4-yl)-1H-benzo[d]imidazole-2,4-dicarboxamide (**9e**)*

Compound **9e** was obtained as a white solid (70 mg, 29.2%); mp

259–261 °C; ^{1}H NMR (400 MHz, DMSO-d_6) δ (ppm): 13.67 (s, 1H), 9.17 (brs, 2H), 7.93 (d, J = 7.2 Hz, 1H), 7.82 (s, 1H), 7.68 (d, J = 7.2 Hz, 1H), 7.41 (t, J = 8.0 Hz, 1H), 4.00–4.09 (m, 2H), 2.70–3.40 (m, 5H), 1.96 (brs, 4H), 1.64 (brs, 2H), 0.88 (t, J = 7.2 Hz, 3H); ^{13}C NMR (100 MHz, DMSO-d_6) δ (ppm): 165.66, 157.89, 145.44, 139.73, 134.97, 123.90, 123.82, 123.51, 116.42, 57.33, 50.62, 44.92, 28.43, 16.70, 11.01; HRMS (ESI): *m/z*, calcd. For $C_{17}H_{24}N_5O_2$ $[M + H]^+$ 330.1925, found 330.1921.

*6.2.15. N^2-(1-iso-Propylpiperidin-4-yl)-1H-benzo[d]imidazole-2,4-dicarboxamide (**9f**)*

Compound **9f** was obtained as a white solid (80 mg, 29.3%); mp 295–297 °C; ^{1}H NMR (400 MHz, DMSO-d_6) δ (ppm): 13.70 (s, 1H), 9.36 (brs, 1H), 9.20 (s, 1H), 7.93 (d, J = 7.6 Hz, 1H), 7.80 (s, 1H), 7.70 (d, J = 8.0 Hz, 1H), 7.41 (t, J = 8.0 Hz, 1H), 4.15 (brs, 1H), 3.30–3.50 (m, 3H), 3.05–3.23 (m, 2H), 2.10–2.24 (m, 2H), 2.01–2.09 (m, 2H), 1.28 (d, J = 6.4 Hz, 6H); HRMS (ESI): *m/z*, calcd. For $C_{17}H_{24}N_5O2_4$ $[M + H]^+$330.1925, found 330.1918.

*6.2.16. N^2-(1-iso-Butylpiperidin-4-yl)-1H-benzo[d]imidazole-2,4-dicarboxamide (**9g**)*

Compound **9g** was obtained as a white solid (40 mg, 24.3%); mp 266–268 °C; ^{1}H NMR (400 MHz, DMSO-d_6) δ (ppm): 13.63 (s, 1H), 9.15 (s, 1H), 9.04 (d, J = 6.8 Hz, 1H), 7.92 (d, J = 7.6 Hz, 1H), 7.79 (s, 1H), 7.68 (d, J = 8.0 Hz, 1H), 7.40 (t, J = 7.6 Hz, 1H), 3.85 (brs, 1H), 2.86 (brs, 2H), 2.04 (brs, 2H), 1.94 (brs, 2H), 1.77 (brs, 5H), 0.85 (d, J = 6.4 Hz, 6H); ^{13}C NMR (100 MHz, DMSO-d_6) δ (ppm): 165.65, 157.704, 145.63, 140.09, 134.68, 123.92, 123.84, 123.72, 116.13, 52.04, 45.80, 29.03, 24.16, 20.75; HRMS (ESI): *m/z*, calcd. For $C_{18}H_{26}N_5O_2$ $[M + H]^+$ 344.2081, found 344.2078.

*6.2.17. N^2-(1-(cyclopropylmethyl) piperidin-4-yl)-1H-benzo[d] imidazole-2,4-dicarboxamide (**9h**)*

Compound **9h** was obtained as a white solid (70 mg, 35.1%); mp 262–264 °C; ^{1}H NMR (300 MHz, DMSO-d_6) δ (ppm): 13.63 (brs, 1H), 9.13 (brs, 2H), 7.94 (d, J = 7.5 Hz, 1H), 7.82 (s, 1H), 7.71 (d, J = 7.5 Hz, 1H), 7.42 (t, J = 7.5 Hz, 1H), 4.36 (brs, 1H), 3.15 (brs, 3H), 2.37 (brs, 3H), 1.86 (brs, 4H), 0.90 (brs, 1H), 0.51 (d, J = 6.0 Hz, 2H), 0.16 (brs, 2H); ^{13}C NMR (100 MHz, DMSO-d_6) δ (ppm): 165.67, 157.90, 145.46, 139.75, 134.80, 123.90, 123.82, 123.51, 116.43, 60.00, 50.38, 44.97, 28.44, 5.29, 4.17; HRMS (ESI): *m/z*, calcd. For $C_{18}H_{24}N_5O_2$ $[M + H]^+$ 342.1925, found 342.1920.

*6.2.18. N^2-(1-neo-Pentylpiperidin-4-yl)-1H-benzo[d]imidazole-2,4-dicarboxamide (**9i**)*

Compound **9i** was obtained as a white solid (100 mg, 44.4%); mp 264–266 °C; ^{1}H NMR (400 MHz, DMSO-d_6) δ (ppm): 13.64 (s, 1H), 9.17 (s, 1H), 9.04 (d, J = 7.6 Hz, 1H), 7.94 (d, J = 7.2 Hz, 1H), 7.80 (s, 1H), 7.70 (d, J = 8.0 Hz, 1H), 7.42 (t, J = 7.6 Hz, 1H), 3.86 (brs, 1H), 2.85 (brs, 2H), 2.34 (brs, 2H), 2.10 (brs, 2H), 1.78 (brs, 4H), 0.88 (s, 9H); HRMS (ESI): *m/z*, calcd. For $C_{19}H_{28}N_5O_2$ $[M + H]^+$ 358.2238, found 358.2226.

*6.2.19. N^2-(1-iso-Pentylpiperidin-4-yl)-1H-benzo[d]imidazole-2,4-dicarboxamide (**9j**)*

Compound **9j** was obtained as a white solid (70 mg, 23.8%); mp 264–266 °C; ^{1}H NMR (400 MHz, DMSO- d_6) δ (ppm): 13.65 (brs, 1H), 9.14 (brs, 1H), 9.03 (d, J = 8.0 Hz, 1H), 7.92 (d, J = 7.6 Hz, 1H), 7.79 (s, 1H), 7.69 (d, J = 8.0 Hz, 1H), 7.40 (t, J = 8.0 Hz, 1H), 3.83 (brs, 1H), 2.91 (d, J = 10.0 Hz, 2H), 2.29 (brs, 2H), 1.97 (brs, 2H), 1.69–1.78 (m, 4H), 1.53–1.60 (m,1H), 1.30–1.34 (m, 2H), 0.86 (d, J = 6.4 Hz, 6H); ^{13}C NMR (100 MHz, DMSO- d_6) δ (ppm): 165.64, 157.47, 145.69, 123.83, 123.65, 55.54, 52.04, 46.47, 34.95, 30.74, 25.82, 22.50; HRMS (ESI): *m/z*, calcd. For $C_{19}H_{28}N_5O_2$ $[M + H]^+$ 358.2238, found 358.2231.

*6.2.20. N^2-(1-(Pentan-3-yl) piperidin-4-yl)-1H-benzo[d]imidazole-2,4-dicarboxamide (**9k**)*

Compound **9k** was obtained as a white solid (60 mg, 28.7%); mp 240–242 °C; ^{1}H NMR (400 MHz, DMSO-d_6) δ (ppm): 13.62 (s, 1H), 9.16 (s, 1H), 9.06 (brs, 1H), 7.92 (d, J = 7.6 Hz, 1H), 7.78 (s, 1H), 7.68 (d, J = 7.6 Hz, 1H), 7.40 (t, J = 7.6 Hz, 1H), 3.82 (brs, 1H), 2.72 (brs, 2H), 2.34 (brs, 2H), 2.18 (brs, 1H), 1.78 (brs, 2H), 1.67 (brs, 2H), 1.44 (brs, 2H), 1.25 (brs, 2H), 0.87 (s, 6H); HRMS (ESI): *m/z*, calcd. For $C_{19}H_{28}N_5O_2$ $[M + H]^+$ 358.2238, found 358.2232.

*6.2.21. N^2-(1-cyclohexylpiperidin-4-yl)-1H-benzo[d]imidazole-2,4-dicarboxamide (**9l**)*

Compound **9l** was obtained as a white solid (90 mg, 29.4%); mp 271–273 °C; ^{1}H NMR (400 MHz, DMSO- d_6) δ (ppm): 13.61 (brs, 1H), 9.14 (brs, 1H), 9.03 (d, J = 8.4 Hz, 1H), 7.92 (d, J = 7.6 Hz, 1H), 7.79 (s, 1H), 7.69 (d, J = 8.0 Hz, 1H), 7.40 (t, J = 7.6 Hz, 1H), 3.81 (brs, 1H), 2.89 (d, J = 9.6 Hz, 2H), 2.33 (bs, 3H), 1.67–1.82 (m, 8H), 1.56 (d, J = 9.6 Hz, 1H), 1.06–1.19 (m, 5H); HRMS (ESI): *m/z*, calcd. For $C_{20}H_{28}N_5O_2$ $[M + H]^+$ 370.2238, found 370.2233.

*6.2.22. tert-Butyl 4-(4-carbamoyl-1H-benzo[d]imidazole-2-carboxamido)1,4'-bipiperidine-1'-carboxylate (**9m**)*

Compound **9m** was obtained as a white solid (70 mg, 23.8%); mp 239–242 °C; ^{1}H NMR (400 MHz, DMSO-d_6) δ (ppm): 13.62 (s, 1H), 9.15 (s, 1H), 9.03 (d, J = 8.4 Hz, 1H), 7.92 (d, J = 7.6 Hz, 1H), 7.79 (s, 1H), 7.68 (d, J = 7.6 Hz, 1H), 7.40 (t, J = 7.6 Hz, 1H), 3.95 (d, J = 11.2 Hz, 2H), 3.82 (brs, 1H), 2.89 (d, J = 10.0 Hz, 2H), 2.69 (brs, 2H), 2.44–2.49 (m, 1H), 2.24 (t, J = 10.4 Hz, 2H), 1.79–1.82 (m, 2H), 1.60–1.71 (m, 4H), 1.38 (s, 9H), 1.22–1.31 (m, 2H); ^{13}C NMR (100 MHz, DMSO-d_6) δ (ppm): 165.62, 157.69, 153.68, 145.63, 140.08, 134.66, 123.88, 116.09, 78.77, 61.56, 47.71, 29.94, 28.04, 26.83; HRMS (ESI): *m/z*, calcd. For $C_{24}H_{35}N_6O_4$ $[M + H]^+$ 471.2714, found 471.2712.

*6.2.23. N^2-(1,4'-Bipiperidine-4-yl) 1H-benzo[d]imidazole-2,4-dicarboxmide 2,2,2-trifluoroacetate (**9n**)*

The title compound was synthesized from **9m** using the same method as the preparation of compound **7c**: Compound **9n** was obtained as a white solid (137 mg, 82%); mp 206–208 °C; ^{1}H NMR (400 MHz, DMSO-d_6) δ (ppm): 10.16 (brs, 1H), 9.30 (d, J = 7.6 Hz, 1H), 9.10 (brs, 1H), 8.95 (brs, 1H), 8.69 (brs, 1H), 7.94 (d, J = 7.2 Hz, 1H), 7.84 (s, 1H), 7.72 (d, J = 8.0 Hz, 1H), 7.42 (t, J = 8.0 Hz, 1H), 4.10–4.17 (m, 2H), 3.46–3.55 (m, 4H), 3.16–3.21 (m, 2H), 2.95 (q, J = 11.2 Hz, 2H), 2.11–2.24 (m, 4H), 1.97 (q, J = 12.4 Hz, 2H), 1.85 (q, J = 11.2 Hz, 2H); HRMS (ESI): *m/z*, calcd. For $C_{19}H_{27}N_6O_2$ $[M + H]^+$ 371.2190, found 371.2181.

*6.2.24. N^2-(Piperidin-4-yl)-1H-benzo[d]imidazole-2,4-dicarboxamide 2,2,2-trifluoroacetate (**9o**)*

The title compound was synthesized from **9a** using the same method as the preparation of compound **7c**: Compound **9o** was obtained as a white solid (50 mg, 56.8%); mp 252–254; ^{1}H NMR (300 MHz, DMSO-d_6) δ (ppm): 13.69 (s, 1H), 9.24 (d, J = 7.5 Hz, 1H), 9.16 (s, 1H), 8.85 (brs, 1H), 8.40 (brs, 1H), 7.93 (d, J = 7.2 Hz, 1H), 7.84 (brs, 1H), 7.70 (d, J = 7.5 Hz, 1H), 7.42 (t, J = 7.8 Hz, 1H), 4.08–4.20 (m, 1H), 3.34–3.44 (m, 2H), 2.98–3.10 (m, 2H), 1.99–2.18 (m, 2H), 1.73–1.95 (m, 2H); HRMS (ESI): *m/z*, calcd. For $C_{14}H_{18}N_5O_2$ $[M + H]^+$ 288.1455, found 288.1451.

*6.2.25. 6-Fluoro-N^2-(1-neo-pentylpiperidin-4-yl)-1H-benzo[d] imidazole-2,4-dicarboxamide (**10a**)*

A mixture of 6-fluoro-2-carboxyl-1*H*-benzo[*d*]immidazole-4-carboxamide (113 mg, 0.50 mmol), HBTU (379 mg, 1.0 mmol), HOBt (135 mg, 1.0 mmol), DIEA (0.35 mL, 2.0 mmol) and 1-neopentylpiperidin-4-amine (170 mg, 1.0 mmol) in DMF (10 mL)

was stirred at room temperature for 20 h and then H_2O was added to the mixture. The solution was extracted with the solvent mixture (ethyl acetate/methanol = 10:1) (30 mL × 3) and then the organic layer was washed with brine (20 mL × 2). The combined organic layer was dried over anhydrous $MgSO_4$. After filtration and concentration, the crude product was obtained and purified with column chromatography (methylene chloride/methanol = 60:1 to 20:1) to give compound **10a** as a white solid (70 mg, 37.2%); mp 261–263 °C; ^{1}H NMR (400 MHz, DMSO-d_6) δ (ppm): 13.76 (s, 1H), 9.15 (s, 1H), 9.03 (d, J = 8.4 Hz, 1H), 7.99 (s, 1H), 7.65 (d, J = 10.4 Hz, 1H), 7.42 (d, J = 8.0 Hz, 1H), 3.83 (brs, 1H), 2.78 (brs, 2H), 2.30 (brs, 2H), 2.06 (brs, 2H), 1.74 (brs, 4H), 0.84 (s, 9H); HRMS (ESI): *m/z*, calcd. For $C_{19}H_{27}N_5O_2F$ $[M + H]^+$ 376.2143, found 376.2142.

6.2.26. 6-Fluoro-N^2-(1-(pentan-3-yl) piperidin-4-yl)-1H-benzo[d] imidazole-2,4-dicarboxamide (**10b**)

The title compound was synthesized from 6-fluoro-2-carboxyl-1*H*-benzo[*d*]immidazole-4- carboxamide using the same method as the preparation of compound **10a**: Compound **10b** was obtained as a white solid (45 mg, 27.2%); mp 268–270 °C; ^{1}H NMR (400 MHz, DMSO-d_6) δ (ppm): 13.80 (s, 1H), 10.02 (brs, 1H), 9.32 (brs, 1H), 9.18 (s, 1H), 8.04 (s, 1H), 7.68 (d, J = 8.0 Hz, 1H), 7.46 (d, J = 7.2 Hz, 1H), 4.18 (brs, 1H), 3.40 (brs, 2H), 3.20 (brs, 2H), 2.98 (brs, 1H), 2.03–2.20 (m, 4H), 1.90 (brs, 2H), 1.60 (brs, 2H), 0.98 (brs, 6H); HRMS (ESI): *m/z*, calcd. For $C_{19}H_{27}N_5O_2F$ $[M + H]^+$ 376.2143, found 376.2142.

6.2.27. tert-Butyl (1-(4-carbomoyl-1H-benzo[d]imidazole-2-carbonyl)pyrrolidin-3-yl)carbamate (**11a**)

Compound **11a** was obtained as a white solid (505 mg, 39.49%); mp. 246–248 °C; Compound **11a** exists as a mixture of two conformers; ^{1}H NMR (400 MHz, DMSO-d_6) δ (ppm): 13.61 (s, 1H), 8.93 (s, 0.5H), 8.88 (s, 0.5H),7.93 (d, J = 7.6 Hz, 1H), 7.82 (d, J = 7.6 Hz, 1H), 7.72 (d, J = 8.0 Hz, 1H), 7.44 (t, J = 7.6 Hz, 1H), 7.26 (brs, 1H), 4.04–4.24 (m, 3H), 3.49–3.75 (m, 2H), 2.13–2.18 (m, 0.5 H), 2.03–2.08 (m, 0.5H), 1.93–1.95 (m, 0.5H), 1.83–1.85 (m, 0.5H), 1.38 (d, J = 11.2 Hz, 9H); ^{13}C NMR (100 MHz, DMSO-d_6) δ (ppm): 165.75, 157.26 (157.18), 155.32 (155.19), 146.25 (146.10), 140.23, 133.75, 124.07, 123.82, 116.15, 77.99, 53.71 (52.65), 50.82 (48.22), 46.98 (45.33), 31.65 (29.06), 28.21; HRMS (ESI): *m/z*, calcd. For $C_{18}H_{24}N_5O_4$ $[M + H]^+$ 374.1823, found 374.1816.

6.2.28. 2-(3-Aminopyrrolidine-1-carbonyl)-1H-benzol[d] imidazole-4-carboxamide 2,2,2-trifluoroacetate (**11b**)

The title compound was synthesized from **11a** using the same method as the preparation of compound **7c**: Compound **11b** was obtained as a white solid (415 mg, 75.3%); mp 226–228 °C; ^{1}H NMR (400 MHz, DMSO-d_6) δ (ppm): 13.71 (brs, 1H), 8.78 (brs, 0.5H), 8.68 (brs, 0.5H), 8.17 (brs, 2H), 7.93–7.97 (m, 1H), 7.75–7.88 (m, 2H), 7.45 (t, J = 7.6 Hz, 1H), 4.31–4.37 (m, 2H), 3.99 (brs, 0.5H), 3.93 (brs, 0.5H), 3.71–3.83 (m, 2H), 2.31–2.40 (m, 0.5H), 2.20–2.30 (m, 0.5H), 2.11–2.19 (m, 0.5H), 2.00–2.10 (m, 0.5H); HRMS (ESI): *m/z*, calcd. For $C_{13}H_{16}N_5O_2$ $[M + H]^+$ 274.1299, found 274.1294.

6.2.29. 2-(3-(Propylamino)pyrrolidine-1-carbonyl)-1H-benzol[d] imidazole-4-carboxamide (**11c**)

To a solution of **11b** (65 mg, 0.13 mmol) in THF (5 mL), DIEA and propionaldehyde (0.03 mL, 0.42 mmol) were added at −40 °C. The reaction mixture was stirred at −40 °C for 30 min. Sodium triacetoxyborohyride ($NaBH(OAc)_3$, 178 mg, 0.84 mmol) was added to the mixture and stirred at −30 °C for 1.5 h, then H_2O (15 mL) was added to the mixture. The solution was extracted with the solvent mixture (ethyl acetate/methanol = 10:1) (15 mL × 6) and then the organic layer dried over anhydrous $MgSO_4$. After filtration and concentration, the crude product was obtained and purified with column chromatography (methylene chloride/methanol = 12.5:1 to 5:1) to give compound **11c** as a white solid (23 mg, 56.1%); mp 242–244 °C; Compound **11c** exists as a mixture of two conformers; ^{1}H NMR (300 MHz, DMSO-d_6) δ (ppm): 8.82 (brs, 1H), 7.94 (d, J = 6.9 Hz, 1H), 7.84 (d, J = 7.5 Hz, 1H), 7.76 (d, J = 7.8 Hz, 1H), 7.44 (t, J = 7.5 Hz, 1H), 4.18–4.38 (m, 2H), 3.67–3.84 (m, 3H), 2.66–2.80 (m, 2H), 1.93–2.30 (m, 2H), 1.47–1.59 (m, 2H), 0.90 (q, J = 6.6 Hz, 3H); ^{13}C NMR (100 MHz, DMSO-d_6) δ (ppm): 165.83, 157.21 (157.10), 145.87 (145.75), 124.27, 124.04, 123.95, 116.60, 57.05 (54.49), 50.58 (49.22), 47.29, 46.62 (45.11), 28.53 (25.59), 19.19, 10.99; HRMS (ESI): *m/z*, calcd. For $C_{16}H_{22}N_5O_2$ $[M + H]^+$ 316.1768, found 316.1765.

6.2.30. 2-(3-Propionamidopyrrolidine-1-carbonyl)-1H-benzol[d] imidazole-4-carboxamide (**11d**)

To a solution of **11b** (65 mg, 0.13 mmol) in DCM (5 mL), DIEA (0.15 mL, 0.84 mmol) and propionyl chloride (0.02 mL, 0.2 mmol) were added at 0 °C. The reaction mixture was stirred at 0 °C for 3 h and then was evaporated. The residue was dissolved with the solvent mixture (ethyl acetate/methanol = 10:1) (40 mL). The organic layer was washed with brine (15 mL × 2) and then the organic layer dried over anhydrous $MgSO_4$. After filtration and concentration, the crude product was obtained and purified with column chromatography (methylene chloride/methanol = 30:1) to give compound **11d** as a white solid (28 mg, 65%); mp 282–284 °C; Compound **11d** exists as a mixture of two conformers. ^{1}H NMR (400 MHz, DMSO-d_6) δ (ppm): 13.63 (s, 1H), 8.94 (s, 0.5 H), 8.87 (s, 0.5H), 8.09 (t, J = 8.4 Hz, 1H), 7.93 (d, J = 7.2 Hz, 1H), 7.83 (s, 1H), 7.73 (d, J = 8.0 Hz, 1H), 7.44 (t, J = 7.6 Hz, 1H), 4.05–4.46 (m, 3H), 3.49–3.79 (m, 2H), 2.03–2.16 (m, 3H), 1.91–2.00 (m, 0.5H), 1.79–1.90 (m, 0.5H), 0.94–1.00 (m, 3H); ^{13}C NMR (100 MHz, DMSO-d_6) δ (ppm): 172.97 (172.88), 165.81, 157.19 (157.09), 146.16 (146.07), 123.95, 123.80, 116.40, 53.79 (52.58), 49.49 (46.96), 46.79 (45.35), 31.73 (28.95), 28.30, 9.81; HRMS (ESI): *m/z*, calcd. For $C_{16}H_{20}N_5O_3$ $[M + H]^+$ 330.1561, found 330.1556.

6.2.31. 2-(3-(Cyclohexylamino)pyrrolidine-1-carbonyl)-1H-benzol [d]imidazole-4-carboxamide (**11e**)

To a solution of **11b** (100 mg, 0.20 mmol) in THF (5 mL), DIEA and cyclohexanone were added. The reaction mixture was stirred at room temperature for 4 d. Sodium triacetoxyborohyride ($NaBH(OAc)_3$, 274 mg, 1.29 mmol) was added to the mixture and stirred at room temperature for 2 h, then H_2O (15 mL) was added to the mixture. The solution was extracted with the solvent mixture (ethyl acetate/methanol = 10:1) (30 mL × 6) and then the organic layer was dried over anhydrous $MgSO_4$. After filtration and concentration, the crude product was obtained and purified with column chromatography (methylene chloride/methanol = 15:1 to 10:1) to give compound **11e** as a white solid (30 mg, 32.7%); mp 233–235 °C;^{1}H NMR (400 MHz, DMSO-d_6) δ (ppm): 8.89 (brs, 1H), 7.94 (d, J = 7.2 Hz, 1H), 7.86 (s, 0.5H), 7.83 (s, 0.5H), 7.75 (brs, 1H), 7.44 (t, J = 7.6 Hz, 1H), 4.34–4.43 (m, 1H), 4.15–4.18 (m, 1H), 3.80–3.87 (m, 2H), 3.58–3.64 (m, 1H), 3.41–3.43 (m, 1H), 2.19–2.28 (m, 2H), 1.99 (brs, 2H), 1.73 (brs, 2H), 1.58 (brs, 2H), 1.04–1.14 (m, 5H); HRMS (ESI): *m/z*, calcd. For $C_{19}H_{26}N_5O_2$ $[M + H]^+$ 356.2081, found 356.2075.

6.2.32. tert-Butyl 4-(1-(4-carbomoyl-1H-benzo[d]imidazole-2-carbonyl)pyrrolidin-3-ylamino)piperidine-1-carboxylate (**11f**)

To a solution of **11b** (150 mg, 0.30 mmol) in THF (10 mL), DIEA and *N*-(*tert*-butoxycarbonyl)-4-piperidone (386 mg, 1.94 mmol) were added. The reaction mixture was stirred at room temperature for 4 d. Sodium triacetoxyborohyride ($NaBH(OAc)_3$, 419 mg, 1.94 mmol) was added to the mixture and stirred at room temperature for 2 h, then H_2O (15 mL) was added to the mixture. The solution was extracted with the solvent mixture (ethyl acetate/methanol = 10:1) (30 mL × 4) and then the organic layer was dried

over anhydrous $MgSO_4$. After filtration and concentration, the crude product was obtained and purified with column chromatography (methylene chloride/methanol = 15:1 to 12.5:1) to give compound **11f** as a white solid (120 mg, 87.7%); mp 209–211 °C; ^{1}H NMR (400 MHz, DMSO-d_6) δ (ppm): 9.55 (brs, 2H), 8.89 (s, 0.5H), 8.84 (s, 0.5H), 7.94 (d, J = 7.2 Hz, 1H), 7.85 (s, 1H), 7.74 (d, J = 8.0 Hz, 1H), 7.45 (t, J = 7.6 Hz, 1H), 4.21–4.55 (m, 2H), 3.88–3.99 (m, 4H), 3.60–3.65 (m, 1H), 3.10–3.40 (m, 1H), 2.78 (brs, 2H), 2.22–2.48 (m, 2H), 2.06 (brs, 2H), 1.40–1.52 (m, 2H), 1.39 (brs, 9H); HRMS (ESI): *m/z*, calcd. For $C_{23}H_{33}N_6O_4$ $[M + H]^+$ 457.2558, found 457.2546.

6.2.33. 2-(3-(Piperidin-4-ylamino)pyyrrolidine-1-carbonyl)-1H-benzo[d]imidazole-4-carboxamide 2,2,2-trifluoroacetate (**11g**)

The title compound was synthesized from **11f** using the same method as the preparation of compound **7c**: Compound **11g** was obtained as a white solid (40 mg, 72.7%); mp 199–201 °C; ^{1}H NMR (400 MHz, DMSO-d_6) δ (ppm): 13.70 (brs, 1H), 9.54 (brs, 2H), 8.95 (brs, 1H), 8.83 (brs, 2H), 7.94 (d, J = 7.6 Hz, 1H), 7.85 (brs, 1H), 7.75 (brs, 1H), 7.46 (t, J = 8.0 Hz, 1H), 4.35–4.60 (m, 2H), 3.85–4.25 (m, 4H), 3.62–3.69 (m, 1H), 3.50 (brs, 1H), 2.94 (brs, 2H), 2.15–2.48 (m, 4H), 1.75–1.90 (m, 2H); HRMS (ESI): *m/z*, calcd. For $C_{18}H_{25}N_6O_4$ $[M + H]^+$ 357.2034, found 357.2027.

6.2.34. tert-Butyl (1-(4-carbomoyl-6-fluoro-1H-benzo[d]imidazole-2-carbonyl)pyrrolidin-3-yl)carbamate (**12a**)

The title compound was synthesized from 6-fluoro-2-carboxyl-1*H*-benzo[*d*]immidazole-4-carboxamide using the same method as the preparation of compound **10a**: Compound **12a** was obtained as a white solid (120 mg, 18%); mp 252–254 °C; ^{1}H NMR (400 MHz, DMSO-d_6) δ (ppm): 13.70 (s, 1H), 8.84 (d, J = 8.8 Hz, 1H), 8.25 (d, J = 7.2 Hz, 1H), 7.68 (d, J = 7.2 Hz, 1H), 7.50 (d, J = 7.2 Hz, 1H), 7.26 (brs, 1H), 4.02–4.30 (m, 3H), 3.58–3.78 (m, 1.5H), 3.48–3.54 (m, 0.5H), 2.12–2.22 (m, 0.5H), 2.02–2.10 (m, 0.5H), 1.90–1.98 (m, 0.5H), 1.82–1.89 (m, 0.5H), 1.39 (d, J = 10.4 Hz, 9H); HRMS (ESI): *m/z*, calcd. For $C_{18}H_{23}N_5O_4F$ $[M + H]^+$ 392.1729, found 392.1723.

6.2.35. 2-(3-Aminopyrrolidine-1-carbonyl)-6-fluoro-1H-benzol[d]imidazole-4-carboxamide 2,2,2-trifluoroacetate (**12b**)

The title compound was synthesized from **12a** using the same method as the preparation of compound **7c**: Compound **12b** was obtained as a white solid (180 mg, 70.5%); mp 244–246 °C; ^{1}H NMR (400 MHz, DMSO-d_6) δ (ppm): 13.80 (s, 1H), 8.84 (s, 0.5H), 8.74 (s, 0.5H), 8.05–8.16 (m, 4H), 7.68 (d, J = 7.6 Hz, 1H), 7.50 (d, J = 8.0 Hz, 1H), 4.25–4.40 (m, 2H), 3.90–4.15 (m, 1H), 3.65–3.86 (m, 2H), 2.30–2.40 (m, 0.5H), 2.20–2.29 (m, 0.5H), 2.15 (brs, 0.5H), 2.05 (brs, 0.5H); HRMS (ESI): *m/z*, calcd. For $C_{13}H_{14}N_5O_2F$ $[M + H]^+$ 292.1204, found 292.1201.

6.2.36. 2-(3-(Cyclohexylamino)pyrrolidine-1-carbonyl)-6-fluoro-1H-benzol[d]imidazole-4-carboxamide (**12c**)

The title compound was synthesized from **12b** using the same method as the preparation of compound **11e**: Compound **12c** was obtained as a white solid (87 mg, 79%); mp 256–258 °C; ^{1}H NMR (400 MHz, DMSO-d_6) δ (ppm): 8.82 (s, 0.5H), 8.76 (s, 0.5H), 8.15 (s, 0.5H), 8.09 (s, 0.5H), 7.68 (d, J = 10.0 Hz, 1H), 7.52 (d, J = 5.2 Hz, 1H), 4.40–4.45 (m, 0.5H), 4.32–4.36 (m, 0.5H), 4.15–4.17 (m, 1H), 3.76–3.91 (m, 2H), 3.67–3.71 (m, 0.5H), 3.57–3.64 (m, 0.5H), 3.01 (brs, 0.5H), 2.91 (brs, 0.5H), 1.99–2.31 (m, 4H), 1.73 (brs, 2H), 1.58 (brs, 1H), 1.08–1.47 (m, 5H); HRMS (ESI): *m/z*, calcd. For $C_{19}H_{25}N_5O_2F$ $[M + H]^+$ 374.1987, found 374.1987.

6.2.37. tert-Butyl (1-(4-carbomyl-1H-benzo[d]imidazole-2-carbonyl)piperidin-4-yl)carbamate (**13a**)

Compound **13a** was obtained as a white solid (140 mg, 37.1%); mp 278–280 °C; ^{1}H NMR (300 MHz, DMSO-d_6) δ (ppm): 13.66 (s, 1H), 9.14 (s, 1H), 9.08 (s, 0.5H), 9.05 (s, 0.5H), 7.93 (d, J = 6.9 Hz, 1H), 7.82 (s, 1H), 7.69 (d, J = 7.8 Hz, 1H), 7.41 (t, J = 7.5 Hz, 1H), 3.97–4.10 (m, 3H), 2.84 (bs, 2H), 1.79–1.82 (m, 2H), 1.49–1.61 (m, 2H), 1.41 (s, 9H); ^{13}C NMR (100 MHz, DMSO-d_6) δ (ppm): 165.63, 157.34, 153.81, 145.67, 140.07, 134.65, 123.88, 123.75, 116.07, 78.64, 46.52, 43.15, 31.18, 28.08; HRMS (ESI): *m/z*, calcd. For $C_{19}H_{26}N_5O_4$ $[M + H]^+$ 388.1979, found 388.1971.

6.2.38. 2-(4-Aminopiperidine-1-carbonyl)-1H-benzol[d]imidazole-4-carboxamide 2,2,2-trifluoroacetate (**13b**)

The title compound was synthesized from **13a** using the same method as the preparation of compound **7c**: Compound **13b** was obtained as a white solid (60 mg, 70.5%); mp 275–277 °C; ^{1}H NMR (300 MHz, DMSO-d_6) δ (ppm): 13.65 (s, 1H), 9.24 (d, J = 7.5 Hz, 1H), 9.17 (s, 1H), 8.64 (brs, 2H), 7.93 (d, J = 7.2 Hz, 1H), 7.84 (s, 1H), 7.70 (d, J = 8.1 Hz, 1H), 7.42 (t, J = 7.5 Hz, 1H), 4.20–4.42 (m, 1H), 3.33–3.38 (m, 2H), 3.06 (t, J = 13.2 Hz, 2H), 1.99–2.09 (m, 2H), 1.82–1.92 (m, 2H); ^{13}C NMR (100 MHz, DMSO-d_6) δ (ppm): 165.69, 157.80, 145.52, 139.99, 134.69, 123.92, 116.18, 109.30, 44.62, 42.45, 28.24; HRMS (ESI): *m/z*, calcd. For $C_{14}H_{18}N_5O_2$ $[M + H]^+$ 288.1455, found 288.1450.

6.2.39. 2-(4-(Cyclohexylamino)piperidine-1-carbonyl)-1H-benzol[d]imidazole-4-carboxamide (**13c**)

The title compound was synthesized from **13b** using the same method as the preparation of compound **11e**: Compound **13c** was obtained as a white solid (45 mg, 42%); mp 228–230 °C;^{1}H NMR (400 MHz, DMSO-d_6) δ (ppm): 8.80 (s, 1H), 7.92 (d, J = 7.6 Hz, 1H), 7.78 (s, 1H), 7.76 (d, J = 8.4 Hz, 1H), 7.42 (t, J = 7.6 Hz, 1H), 4.80 (d, J = 13.2 Hz, 1H), 4.39 (d, J = 12.8 Hz, 1H), 3.41 (t, J = 11.6 Hz, 1H), 3.05 (t, J = 11.6 Hz, 1H), 2.97–2.99 (m, 1H), 2.59 (t, J = 10.0 Hz, 1H), 1.89–1.95 (m, 2H), 1.83 (d, J = 11.2 Hz, 2H), 1.67 (d, J = 12.8 Hz, 2H), 1.56 (d, J = 12.0 Hz, 1H), 0.97–1.38 (m, 7H); ^{13}C NMR (100 MHz, DMSO-d_6) δ (ppm): 165.98, 158.14, 146.21, 123.70, 123.60, 123.44, 122.81, 117.07, 52.14, 49.99, 44.92, 41.12, 32.20, 32.07, 31.28, 25.59, 24.38; HRMS (ESI): *m/z*, calcd. For $C_{20}H_{28}N_5O_2$ $[M + H]^+$ 370.2238, found 370.2235.

6.2.40. tert-Butyl 4-(1-(4-carbomoyl-1H-benzo[d]imidazole-2-carbonyl)piperidin-4-ylamino)piperidine-1-carboxylate (**13d**)

The title compound was synthesized from **13b** using the same method as the preparation of compound **11f**: Compound **13d** was obtained as a white solid (100 mg, 72.9%); mp 221–223 °C; ^{1}H -NMR (400 MHz, DMSO-d_6) δ (ppm): 8.76 (brs. 1H), 7.91 (d, J = 7.6 Hz, 1H), 7.78 (s, 1H), 7.74 (d, J = 8.0 Hz, 1H), 7.41 (t, J = 7.6 Hz, 1H), 4.78 (d, J = 12.8 Hz, 1H), 4.36 (d, J = 12.8 Hz, 1H), 3.83 (d, J = 12.8 Hz, 2H), 3.42 (t, J = 11.6 Hz, 1H), 3.06 (t, J = 11.6 Hz, 1H), 2.94 (brs, 1H), 2.76 (brs, 3H), 1.91 (t, J = 10.4 Hz, 2H), 1.77 (d, J = 12.0 Hz, 2H), 1.22–1.38 (m, 11H), 1.05–1.58 (m, 2H); HRMS (ESI): *m/z*, calcd. For $C_{24}H_{35}N_6O_4$ $[M + H]^+$ 471.2714, found 471.2708.

6.2.41. 2-(4-(Piperidin-4-ylamino)piperidine-1-carbonyl)-1H-benzo[d]imidazole-4-carboxamide 2,2,2-trifluoroacetate (**13e**)

The title compound was synthesized from **13d** using the same method as the preparation of compound **7c**: Compound **13e** was obtained as a white solid (88 mg, 77.8%); mp 171–173 °C; ^{1}H NMR (400 MHz, DMSO-d_6) δ (ppm): 8.98 (brs, 1H), 8.83 (brs, 1H), 8.66 (brs, 1H), 7.93 (d, J = 7.2 Hz, 1H), 7.85 (brs, 1H), 7.61 (brs, 1H), 7.44 (t, J = 7.6 Hz, 1H), 5.18 (brs, 1H), 4.64 (d, J = 13.2 Hz, 1H), 3.61 (brs, 1H), 3.51 (brs, 1H), 3.41 (d, J = 12.0 Hz, 2H), 3.32 (t, J = 12.8 Hz, 1H), 2.92–2.99 (m, 3H), 2.10–2.20 (m, 4H), 1.52–1.74 (m, 4H); HRMS (ESI): *m/z*, calcd. For $C_{19}H_{27}N_6O_2$ $[M + H]^+$ 371.2190, found 371.2184.

*6.2.42. tert-Butyl (1-(4-carbomyl-6-fluoro-1H-benzo[d]imidazole-2-carbonyl)piperidin-4-yl)carbamate (**14a**)*

The title compound was synthesized from 6-fluoro-2-carboxyl-1*H*-benzo[*d*]immidazole-4-carboxamide using the same method as the preparation of compound **10a**: Compound **14a** was obtained as a white solid (177 mg, 44.5%); mp 262–264 °C; ^{1}H NMR (400 MHz, DMSO-d_6) δ (ppm): 13.73 (s, 1H), 8.77 (s, 1H), 8.02 (s, 1H), 7.66 (d, J = 8.0 Hz, 1H), 7.52 (d, J = 8.0 Hz, 1H), 6.95 (d, J = 7.6 Hz, 1H), 4.85 (d, J = 11.2 Hz, 1H), 4.40 (d, J = 11.2 Hz, 1H), 3.63 (brs, 1H), 3.46 (t, J = 11.2 Hz, 1H), 3.08 (t, J = 11.2 Hz, 1H), 1.78 (brs, 2H), 1.39–1.50 (m, 11H); ^{13}C NMR (100 MHz, DMSO-d_6) δ (ppm): 165.35, 159.11 (d, J_{CF} = 237.7), 157.56, 154.79, 146.78, 136.40, 134.02, 124.99, 111.65 (d, J_{CF} = 27.4), 101.96 (d, J_{CF} = 27.6), 77.65, 46.92, 45.13, 41.42, 32.38, 31.57, 28.23; HRMS (ESI): *m/z*, calcd. For $C_{19}H_{25}N_5O_4F$ $[M + H]^+$ 406.1885, found 406.1880.

*6.2.43. 2-(4-Aminopiperidine-1-carbonyl)-6-fluoro-1H-benzol[d]imidazole-4-carboxamide 2,2,2-trifluoroacetate (**14b**)*

The title compound was synthesized from **14a** using the same method as the preparation of compound **7c**: Compound **14b** was obtained as a white solid (150 mg, 78.9%); mp 231–233 °C; ^{1}H NMR (400 MHz, DMSO-d_6) δ (ppm): 13.80 (s, 1H), 8.69 (s, 1H), 8.01 (brs, 4H), 7.66 (d, J = 8.0 Hz, 1H), 7.55 (brs, 1H), 5.01 (brs, 1H), 4.54 (d, J = 13.2 Hz, 1H), 3.30–3.48 (m, 2H), 2.98 (t, J = 12.4 Hz, 1H), 2.03 (t, J = 12.4 Hz, 2H), 1.45–1.48 (m, 2H); HRMS (ESI): *m/z*, calcd. For $C_{14}H_{17}N_5O_2F$ $[M + H]^+$ 306.1361, found 306.1358.

*6.2.44. 2-(4-(Cyclohexylamino)piperidine-1-carbonyl)-6-fluoro-1H-benzol[d]imidazole-4-carboxamide (**14c**)*

The title compound was synthesized from **14b** using the same method as the preparation of compound **11e**: Compound **14c** was obtained as a white solid (37 mg, 42.5%); mp 260–262 °C; ^{1}H NMR (400 MHz, DMSO-d_6) δ (ppm): 8.91 (s, 1H), 7.93 (s, 1H), 7.60 (d, J = 10.0 Hz, 1H), 7.51 (d, J = 8.0 Hz, 1H), 4.70 (d, J = 12.8 Hz, 1H), 4.41 (d, J = 12.4 Hz, 1H), 3.31 (t, J = 12.4 Hz, 1H), 2.95–3.04 (m, 2H), 2.66 (brs, 1H), 1.83–1.96 (m, 5H), 1.66 (d, J = 11.2 Hz, 2H), 1.55 (d, J = 11.2 Hz, 1H), 1.02–1.36 (m, 6H); HRMS (ESI): *m/z*, calcd. For $C_{20}H_{27}N_5O_2F$ $[M + H]^+$ 388.2143, found 388.2142.

*6.2.45. tert-Butyl 4-(4-carbamoyl-1H-benzo[d]imidazole-2-carbonyl)piperazine-1-carboxylate (**15a**)*

Compound **15a** was obtained as a white solid (180 mg, 48.2%); mp 232–233 °C; ^{1}H NMR (400 MHz, DMSO-d_6) δ (ppm): 13.65 (s, 1H), 8.75 (s, 1H), 7.93 (d, J = 7.2 Hz, 1H), 7.77 (s, 1H), 7.73 (d, J = 8.0 Hz, 1H), 7.44 (t, J = 8.0 Hz, 1H), 4.23 (brs, 2H), 3.71 (brs, 2H), 3.47 (brs, 4H), 1.42 (s, 9H); ^{13}C NMR (100 MHz, DMSO-d_6) δ (ppm): 165.65, 158.17.153.81, 145.59, 139.74, 133.68, 123.94, 116.05, 79.28, 46.26, 43.27, 28.04; HRMS (ESI): *m/z*, calcd. For $C_{18}H_{24}N_5O_4$ $[M + H]^+$ 374.1823, found 374.1814.

*6.2.46. (S)-tert-Butyl 4-(4-carbamoyl-1H-benzo[d]imidazole-2-carbonyl)-2-ethylpiperazine-1-carboxylate (**15b**)*

Compound **15b** was obtained as a white solid (210 mg, 50.6%); mp 219–221 °C; Compound **15b** exists as a mixture of two conformers; ^{1}H NMR (400 MHz, DMSO-d_6) δ (ppm): 13.67 (s, 1H), 8.76 (s, 0.5H), 8.72 (s, 0.5H), 7.93 (d, J = 7.2 Hz, 1H), 7.84 (s, 0.5H), 7.72–7.78 (m, 1.5H), 7.44 (t, J = 8.0 Hz, 1H), 5.07 (t, J = 11.2 Hz, 1H), 4.38–4.50 (m, 1H), 3.85–4.15 (m, 2H), 3.52–3.60 (m, 0.5H), 3.30–3.40 (m, 0.5H), 2.95–3.10 (m, 2H), 1.41–1.52 (m, 11H), 0.85 (t, J = 7.2 Hz, 2H), 0.72 (t, J = 7.2 Hz, 1H); ^{13}C NMR (100 MHz, DMSO-d_6) δ (ppm): 165.86, 158.80 (158.65), 153.91 (153.87), 145.58, 123.90, 123.81, 116.92, 79.08, 52.26, 48.23, 46.21, 44.37, 42.36, 27.99, 21.77 (21.64), 10.35 (10.10); HRMS (ESI): *m/z*, calcd. For $C_{20}H_{28}N_5O_4$ $[M + H]^+$ 402.2136, found 402.2128.

*6.2.47. (R)-tert-Butyl 4-(4-carbamoyl-1H-benzo[d]imidazole-2-carbonyl)-2-ethylpiperazine-1-carboxylate (**15c**)*

Compound **15c** was obtained as a white solid (190 mg, 60.7%); mp 208–210 °C; Compound **15c** exists as a mixture of two conformers; ^{1}H NMR (300 MHz, DMSO-d_6) δ (ppm): 13.70 (s, 1H), 8.78 (s, 0.5H), 8.72 (s, 0.5H), 7.94 (d, J = 7.5 Hz, 1H), 7.86 (brs, 0.5H), 7.80 (brs, 0.5H), 7.75 (d, J = 8.4 Hz, 1H), 7.46 (t, J = 7.5 Hz, 1H), 5.04–5.15 (m, 1H), 4.40–4.50 (m, 1H), 4.05–4.14 (m, 1H), 3.84–3.89 (m, 1H), 3.54–3.62 (m, 0.5H), 3.38–3.49 (m, 0.5H), 2.96–3.12 (m, 2H), 1.40–1.60 (m, 11H), 0.86 (t, J = 7.2 Hz, 2H), 0.74 (t, J = 7.2 Hz, 1H); ^{13}C NMR (100 MHz, DMSO-d_6) δ (ppm): 165.87, 158.83 (158.67), 153.94 (153.89), 145.61 (145.56), 139.24, 133.94, 123.93, 123.84, 116.43, 79.11, 52.43, 48.25, 46.22, 44.39, 42.37, 28.01, 21.78 (21.63), 10.37 (10.12); HRMS (ESI): *m/z*, calcd. For $C_{20}H_{28}N_5O_4$ $[M + H]^+$ 402.2136, found 402.2130.

*6.2.48. 2-(4-iso-Butylpiperazine-1-carbonyl)-1H-benzo[d]imidazole-4-carboxamide (**15d**)*

Compound **15d** was obtained as a white solid (30 mg, 18.7%); mp 228–230 °C; ^{1}H NMR (400 MHz, DMSO-d_6) δ (ppm): 13.61 (s, 1H), 8.83 (s, 1H), 7.92 (d, J = 8.4 Hz, 1H), 7.78 (s, 1H), 7.73 (d, J = 7.6 Hz, 1H), 7.44 (t, J = 7.6 Hz, 1H), 4.23 (brs, 2H), 3.76 (brs, 2H), 2.48 (brs, 4H), 2.12 (d, J = 7.2 Hz, 1H), 1.80–1.85 (m, 1H), 0.87 (d, J = 6.4 Hz, 6H); HRMS (ESI): *m/z*, calcd. For $C_{17}H_{24}N_5O_2$ $[M + H]^+$ 330.1925, found 330.1921.

*6.2.49. 2-(Piperazine-1-carbonyl)-1H-benzo[d]imidazole-4-carboxamide 2,2,2-trifluoroacetate (**15e**)*

The title compound was synthesized from **15a** using the same method as the preparation of compound **7c**: Compound **15e** was obtained as a white solid (90 mg, 75%); mp 235–237 °C; ^{1}H NMR (400 MHz, DMSO-d_6) δ (ppm): 13.71 (s, 1H), 8.96 (brs, 2H), 8.64 (brs, 1H), 7.93 (d, J = 7.6 Hz, 1H), 7.79 (brs, 2H), 7.45 (t, J = 7.6 Hz, 1H), 4.51 (brs, 2H), 3.91 (brs, 2H), 3.27 (brs, 4H); ^{13}C NMR (100 MHz, DMSO-d_6) δ (ppm): 165.99, 158.19, 145.25, 123.96, 43.42, 42.86, 42.51; HRMS (ESI): *m/z*, calcd. For $C_{13}H_{16}N_5O_2$ $[M + H]^+$ 274.1299, found 274.1296.

*6.2.50. (S)-2-(3-Ethylpiperazine-1-carbonyl)-1H-benzo[d]imidazole-4-carboxamide 2,2,2-trifluoroacetate (**15f**)*

The title compound was synthesized from **15b** using the same method as the preparation of compound **7c**: Compound **15f** was obtained as a white solid (88 mg, 69.2%); mp 250–252 °C; ^{1}H NMR (400 MHz, DMSO-d_6) δ (ppm): 13.68 (s, 1H), 9.00–9.32 (m, 2H), 8.65 (s, 1H), 7.94 (d, J = 7.2 Hz, 1H), 7.74–7.82 (m, 1H), 7.75 (d, J = 8.0 Hz, 1H), 7.46 (t, J = 7.2 Hz, 1H), 5.59 (d, J = 10.8 Hz, 0.5H), 5.23 (d, J = 12.0 Hz, 0.5H), 4.50–4.60 (m, 1H), 3.82–3.88 (m, 0.5H), 3.06–3.48 (m, 4.5H), 1.50–1.72 (m, 2H), 0.93–1.03 (m, 3H); HRMS (ESI): *m/z*, calcd. For $C_{15}H_{20}N_5O_2$ $[M + H]^+$ 302.1612, found 302.1608.

*6.2.51. (R)-2-(3-Ethylpiperazine-1-carbonyl)-1H-benzo[d]imidazole-4-carboxamide 2,2,2-trifluoroacetate (**15g**)*

The title compound was synthesized from **15c** using the same method as the preparation of compound **7c**: Compound **15g** was obtained as a white solid (90 mg, 70.8%); mp 253–255 °C; ^{1}H NMR (300 MHz, DMSO-d_6) δ (ppm): 13.65 (s, 1H), 9.20 (s, 1H), 9.00 (s, 1H), 8.65 (s, 1H), 7.94 (d, J = 7.2 Hz, 1H), 7.75 (s, 1H), 7.46 (t, J = 7.2 Hz, 1H), 5.58 (brs, 0.5H), 5.20 (brs, 0.5H), 4.50–4.60 (m, 1H), 3.32–3.80 (m, 3H), 3.05–3.30 (m, 2H), 1.50–1.72 (m, 2H), 0.90–1.05 (m, 3H); HRMS (ESI): *m/z*, calcd. For $C_{15}H_{20}N_5O_2$ $[M + H]^+$ 302.1612, found 302.1608.

*6.2.52. N^2-(Quinuclidin-3-yl) 1H-benzo[d]imidazole-2,4-dicarboxmide (**15h**)*

The mixture of 2-carboxyl-1*H*-benzo[*d*]immidazole-4-carboxamide (150 mg, 0.73 mmol), EDC (280 mg, 1.46 mmol), HOBt (1973 mg, 1.46 mmol), DMAP (35 mg, 0.3 mmol), Et_3N (0.63 mL, 4.38 mmol) and 3-aminoquinuclidine dihydrochloride (218 mg, 1.09 mmol) in DMF (10 mL) was stirred at room temperature for 48 h, and then the mixture was evaporated. The crude product was obtained and purified with column chromatography (methylene chloride/methanol/Et_3N = 20:1:0.2 to 8:1:0.08) to give compound **15h** as a white solid (135 mg, 59%); mp 201–203 °C; ^{1}H NMR (400 MHz, DMSO-d_6) δ (ppm): 9.16 (s, 1H), 8.94 (d, J = 6.8 Hz, 1H), 7.94 (d, J = 7.6 Hz, 1H), 7.81 (s, 1H), 7.72 (d, J = 8.0 Hz, 1H), 7.42 (t, J = 8.0 Hz, 1H), 4.04–4.08 (m, 1H), 3.17 (t, J = 12.0 Hz, 1H), 2.95 (t, J = 10.4 Hz, 1H), 2.85 (dd, J_1 = 14.0 Hz, J_2 = 5.6 Hz, 1H), 2.66–2.78 (m, 3H), 1.95 (brs, 1H), 1.80–1.90 (m, 1H), 1.63 (t, J = 6.0 Hz, 1H), 1.36 (t, J = 11.6 Hz, 1H); ^{13}C NMR (100 MHz, DMSO-d_6) δ (ppm): 165.77, 158.58, 145.72, 139.68, 135.36, 123.87, 123.70, 123.39, 116.66, 52.30, 46.64, 46.39, 45.98, 25.54, 24.51, 19.20; HRMS (ESI): *m/z*, calcd. For $C_{16}H_{20}N_5O_2$ $[M + H]^+$ 314.1611, found 314.1605.

*6.2.53. 2-((4aR,7aR)-Octahydro-1H-pyrrolo[3,4-b]pyridine-6-carbonyl)-1H-benzo[d]imidazole-4-carboxamide (**15i**)*

The mixture of 2- carboxyl-1*H*-benzo[*d*]immidazole-4-carboxamide (60 mg, 0.29 mmol), HBTU (222 mg, 0.58 mmol), HOBt (79 mg, 0.58 mmol), Et_3N (0.17 mL, 1.17 mmol) and (S,S)-2,8-Diazabicyclo[4.3.0]nonane (73 mg, 0.58 mmol) in DMF (5.0 mL) was stirred at room temperature for 48 h, and then the mixture was evaporated. The crude product was obtained and purified with column chromatography (methylene chloride/methanol/acetic acid = 4:1:0.05) to give the corresponding product **15i** as a white solid (30 mg, 32.9%); mp 201–203 °C; ^{1}H NMR (400 MHz, DMSO-d_6) δ (ppm): 8.94 (brs, 0.5H), 8.89 (brs, 0.5H), 7.91 (d, J = 7.2 Hz, 1H), 7.74–7.78 (m, 2H), 7.41 (t, J = 7.6 Hz, 1H), 4.01–4.23 (m, 2H), 3.61–3.67 (m, 1H), 3.28 (brs, 0.5H), 3.22 (brs, 0.5H), 2.79–2.91 (m, 2H), 2.44 (brs, 1H), 2.26–2.31 (m, 1H), 1.51–1.74 (m, 3H), 1.38 (brs, 1H); HRMS (ESI): *m/z*, calcd. For $C_{16}H_{20}N_5O_2$ $[M + H]^+$ 314.1611, found 314.1604.

*6.2.54. 2-(3-Oxopiperazine-1-carbonyl)-1H-benzo[d]imidazole-4-carboxamide (**15j**)*

The mixture of 2-carboxyl-1*H*-benzo[*d*]immidazole-4-carboxamide (100 mg, 0.49 mmol), HATU (371 mg, 0.98 mmol), HOAt (133 mg, 0.98 mmol), DIEA (0.34 mL, 1.95 mmol) and piperazin-2-one (98 mg, 0.98 mmol) in DMF(8.0 mL) was stirred at room temperature for 24 h and then the mixture was evaporated. The crude product was obtained and purified with column chromatography (methylene chloride/methanol/Et_3N = 20:1:0.2 to 8:1:0.08) to give compound **15j** as a white solid (80 mg, 57.2%); mp 266–268 °C; Compound **15j** exists as a mixture of two conformers; ^{1}H NMR (400 MHz, DMSO-d_6) δ (ppm): 13.69 (s, 1H), 8.80 (brs, 0.5H), 8.74 (brs, 0.5H), 8.22 (s, 0.5H), 8.18 (s, 0.5H), 7.90–7.98 (m, 1.5H), 7.73–7.82 (m, 1.5H), 7.47 (t, J = 8.4 Hz, 1H), 4.89 (s, 1H), 4.45 (brs, 1H), 4.22 (s, 1H), 3.90 (brs, 1H), 3.40 (s, 2H); ^{13}C NMR (100 MHz, DMSO-d_6) δ (ppm): 165.92, 165.72, 157.90 (157.68), 145.47 (145.40), 123.95, 116.93, 49.90 (46.51), 43.38 (40.32), 39.17; HRMS (ESI): *m/z*, calcd. For $C_{13}H_{14}N_5O_3$ $[M + H]^+$ 288.1091, found 288.1090.

*6.2.55. 2-(4-Propionylpiperazine-1-carbonyl)-1H-benzo[d]imidazole-4-carboxamide (**15k**)*

The title compound was synthesized from **15e** using the same method as the preparation of compound **11d**: Compound **15k** was obtained as a white solid (37 mg, 90.2%); mp 251–253 °C; ^{1}H NMR (400 MHz, DMSO-d_6) δ (ppm): 13.65 (s, 1H), 8.76 (s, 1H), 7.93 (d, J = 7.2 Hz, 1H), 7.75 (brs, 2H), 7.44 (brs, 1H), 4.22–4.29 (m, 2H), 3.69–3.75 (m, 2H), 3.59 (brs, 4H), 2.30–2.52 (m, 2H), 0.99 (brs, 3H); HRMS (ESI): *m/z*, calcd. For $C_{16}H_{20}N_5O_3$ $[M + H]^+$ 330.1561, found 330.1558.

*6.2.56. 6-Fluoro-2-(3-oxopiperazine-1-carbonyl)-1H-benzo[d]imidazole-4-carboxamide (**16a**)*

The mixture of 6-fluoro-2-carboxyl-1*H*-benzo[*d*]immidazole-4-carboxamide (180 mg, 0.8 mmol), HBTU (606 mg, 1.6 mmol), HOBt (216 mg, 1.6 mmol), DIEA (0.56 mL, 3.2 mmol) and piperazin-2-one (160 mg, 1.6 mmol) in DMF (20.0 mL) was stirred at room temperature for 24 h then the mixture was evaporated. The crude product was obtained and purified with column chromatography (methylene chloride/methanol/Et_3N = 20:1:0.2 to 6:1:0.06) to give compound **16a** as a white solid (180 mg, 70%); mp 195–197 °C; ^{1}H NMR (400 MHz, DMSO-d_6) δ (ppm): 13.58 (brs, 1H), 8.68 (brs, 0.5H), 8.62 (brs, 0.5H), 8.18 (d, J = 14.4 Hz, 1H), 8.05 (s, 0.5H), 7.95 (s, 0.5H), 7.69 (d, J = 9.6 Hz, 1H), 7.54 (s, 1H), 4.82 (s, 1H), 4.38 (s, 1H), 4.19 (s, 1H), 3.87 (s, 1H), 3.32 (s, 2H); HRMS (ESI): *m/z*, calcd. For $C_{13}H_{13}N_5O_3F$ $[M + H]^+$ 306.0997, found 306.0996.

*6.2.57. 6-Fluoro-2-(3-oxo-4-(pentan-3-yl)piperazine-1-carbonyl)-1H-benzo[d]imidazole-4-carboxamide (**16b**)*

The title compound was synthesized from 6-fluoro-2-carboxyl-1*H*-benzo[*d*]immidazole-4-carboxamide using the same method as the preparation of compound **16a**: Compound **16b** was obtained as a white solid (60 mg, 30.7%); mp 275–277 °C; ^{1}H NMR (300 MHz, DMSO-d_6) δ (ppm): 13.80 (s, 1H), 8.78 (s, 0.5H), 8.68 (s, 0.5H), 8.12 (s, 0.5H), 8.00 (s, 0.5H), 7.64–7.74 (m, 1H), 7.52 (brs, 1H), 4.96 (s, 1H), 4.50 (s, 1H), 4.20–4.31 (m, 2H), 3.91 (s, 1H), 3.20–3.30 (m, 2H), 1.40–1.52 (m, 4H), 0.79 (t, J = 5.7 Hz, 6H); HRMS (ESI): *m/z*, calcd. For $C_{18}H_{23}N_5O_3F$ $[M + H]^+$ 376.1779, found 376.1777.

Note: Except for target compounds, the synthesis and characterization of all other compounds mentioned in Scheme 1 were described in the supporting information.

6.3. Biological evaluation

6.3.1. The assay for PARP-1 and PARP-2 inhibition

Plasmid pET32a-PARP1 was a gift from Prof. Satoh (Canada). Human recombinant PARP1/2 were expressed and purified as described [30]. The ability of compounds to inhibit PARP1/2 enzyme activity were tested using ELISA method and the chemical quantitation of NAD^+ method as described [30,31]. IC_{50} values were calculated using GraphPad Prism 5 software.

6.3.2. The PF_{50} assay in MX-1 cells

In chemosensitization assays, MX-1 cells were seeded in a density (2000 cells/well) in 96-well plates. Cells were treated with PARP inhibitors at a fixed concentration of 10 μmol/L and temozolomide (TMZ) at different concentrations (0–0.5 mmol/L). After 72 h treatment, cell survival was determined by MTT assay. IC_{50} values were calculated using GraphPad Prism5 software. Potentiation factor (PF_{50}) was calculated as the ratio of the IC_{50} for TMZ divided by the IC_{50} of the combination (TMZ + PARP inhibitor).

6.3.3. Xenograft experiment

Female athymic BALB/c nude mice (8–10 week old) were purchased from Vital River Laboratories, Beijing, China. A total of 1×10^6 MX-1 cells in 0.1 mL sterilized PBS were implanted subcutaneously in mice. After 6 days, the mice were grouped (6 mice/group) with tumor volumes at 100–300 mm^3 and received treatment. TMZ was given by oral gavage once daily for five days at the dose of 50 mg/kg/day and compound **10a** was administered orally once daily at the dose of 50 mg/kg/day for ten days. For

combination groups, both TMZ and compound **10a** were administrated orally once daily for five days. Body weights and tumor volumes were measured twice every week. The mice were euthanized at Day 11. %T/C is calculated as (tumor weight of treatment group/Vehicle or TMZ treatment group) × 100, while %TGI is calculated as (100-%T/C). Statistical analyses were performed by GraphPad Prism5 software and the significance levels were evaluated using one-way ANOVA model.

6.4. The X-ray crystallographic experiment

6.4.1. Protein expression and purification

Human PARP-1 catalytic domain (residues 663–1011, catPARP-1) was cloned to pET-28a (Novagen) to construct the recombinant expression vector. The V762A mutagenesis was carried out on pET28a-PARP-1 with Site-Directed Mutagenesis Kit from Transgen Biotech. The inserted genes were sequenced to ensure the sequence was correct. The expression and purification of wild type and mutant PARP-1 was carried out as previously reported. Generally speaking, upon reaching an optical density (OD600) of 0.5–0.8, the expression of catPARP-1 protein was induced by adding 0.4 mM isopropyl β-D-1-thiogalactopyranoside (IPTG) at 18 °C. Following cell lysis by sonication in lysis buffer (50 mM Tris (pH7.4), 300 mM NaCl and 15 mM imidazole) with EDTA-free protease-inhibitor cocktail (Thermo Scientific), the catPARP-1 protein was first purified using Ni^{2+}-chelating column, followed by ion-exchange (HITRAP SP HP, GE Healthcare) and gel-filtration (SUPERDEX 200, GE Healthcare) purifications. The purified protein was concentrated to 80 mg/mL in stock buffer (50 mM Tris-HCl (pH 7.4), 150 mM NaCl, 5 mM DTT) and stored at −80 °C.

6.4.2. Crystallography

The purified V762A mutant PARP-1 (17 mg/mL) was crystallized by hanging drop vapor diffusion method. The crystals were grown at 18 °C after 5 days. The protein-ligand complex crystals were obtained by soaking apo crystals in reservoir solution (2.45 M $(NH_4)_2SO_4$, 0.1 M Tris, pH 7.5) containing 2 mM of tested compounds. Then crystals were immediately cryoprotected by immersing in the well solution containing 20% v/v glycerol before being flash-frozen in liquid nitrogen. Diffraction data were collected at Shanghai Synchrotron Research Facility (SSRF) using the beam-line BL17U. The data were processed with HKL-3000 software [32]. The PARP-1 structures were primarily determined by molecular replacement using the published PDB structure (PDB code: 4L6S) as the searching model. After initial refinement, the specific compound was modeled into the electron density with COOT software [33]. The structures of the PARP-1 complexed with small molecules were finally refined with restrains using REFMAC5 [34] in CCP4 suite. The structures have been deposited to the Protein Data Bank (PDB) with accession codes: 5WS1 (compound **11b**), 5WS0 (compound **15e**).

Acknowledgements

This work is supported by National Natural Science Foundation of China (No. 81673300) and Special Funds for National Public Benefit Research Institutes (2016ZX350039). We greatly appreciate Dr. Niu Huang and Yanli Wang (National Institute of Biological Sciences, Beijing) for their supports on X-ray crystallographic experiment.

Appendix A. Supplementary data

Supplementary data related to this article can be found at http://dx.doi.org/10.1016/j.ejmech.2017.03.013.

References

[1] J.C. Ame, C. Spenlehauer, G. de Murcia, The PARP superfamily, Bioessays 26 (2004) 882–893.
[2] T. Helleday, Putting poly (ADP-ribose) polymerase and other DNA repair inhibitors into clinical practice, Curr. Opin. Oncol. 25 (2013) 609–614.
[3] M.F. Langelier, J.L. Planck, S. Roy, J.M. Pascal, Structural basis for DNA damage-dependent poly(ADP-ribosyl)ation by human PARP-1, Science 336 (2012) 728–732.
[4] D.V. Ferraris, Evolution of Poly(ADP-ribose) polymerase-1 (PARP-1) inhibitors. From concept to clinic, J. Med. Chem. 53 (2010) 4561–4584.
[5] L. Virág, C. Szabó, The therapeutic potential of poly(ADPribose)polymerase inhibitors, Pharmacol. Rev. 54 (2002) 375–429.
[6] H. Florian, H. Philipp, E.R. Nina, P. Michael, K. Stefan, B. Andreas du, Poly(ADP-ribosyl)ation polymerases: mechanism and new target of anticancer therapy, Expert Rev. Anticancer Ther. 10 (2010) 1125–1136.
[7] M.O. Hottiger, P.O. Hassa, B. Lüscher, H. Schüler, F. Koch-Nolte, Toward a unified nomenclature for mammalian ADP-ribosyltransferases, Trends biochem. Sci. 35 (2010) 208–219.
[8] C.A. Delaney, L.Z. Wang, S. Kyle, A.W. White, A.H. Calvert, N.J. Curtin, B.W. Durkacz, Z. Hostomsky, D.R. Newell, Potentiation of temozolomide and topotecan growth inhibition and cytotoxicity by novel poly(adenosine diphosphoribose) polymerase inhibitors in a panel of human tumor cell lines, Clin. Cancer Res. 6 (2000) 2860–2867.
[9] R.A. Daniel, A.L. Rozanska, E.A. Mulligan, Y. Drew, H.D. Thomas, D.J. Castelbuono, Z. Hostomsky, E.R. Plummer, D.A. Tweddle, A.V. Boddy, S.C. Clifford, N.J. Curtin, Central nervous system penetration and enhancement of temozolomide activity in childhood medulloblastoma models by poly(ADP-ribose) polymerase inhibitor AG-014699, Br. J. Cancer 103 (2010) 1588–1596.
[10] S. Kummar, J. Ji, R. Morgan, H.J. Lenz, S.L. Puhalla, C.P. Belani, D.R. Gandara, D. Allen, B. Kiesel, J.H. Beumer, E.M. Newman, L. Rubinstein, A. Chen, Y. Zhang, L. Wang, R.J. Kinders, R.E. Parchment, J.E. Tomaszewski, J.H. Doroshow, A phase I study of veliparib in combination with metronomic cyclophosphamide in adults with refractory solid tumors and lymphomas, Clin. Cancer Res. 18 (2012) 1726–1734.
[11] B. Evers, R. Drost, E. Schut, M. de Bruin, E. van der Burg, P.W. Derksen, H. Holstege, X. Liu, E. van Drunen, H.B. Beverloo, G.C. Smith, N.M. Martin, A. Lau, M.J. O'Connor, J. Jonkers, Selective inhibition of BRCA2-deficient mammary tumor cell growth by AZD2281 and cisplatin, Clin. Cancer Res. 14 (2008) 3916–3925.
[12] C.K. Donawho, Y. Luo, Y.P. Luo, T.D. Penning, J.L. Bauch, J.J. Bouska, V.D. Bontcheva-Diaz, B.F. Cox, T.L. DeWeese, L.E. Dillehay, D.C. Ferguson, N.S. Ghoreishi-Haack, D.R. Grimm, R. Guan, E.K. Han, R.R. Holley-Shanks, B. Hristov, K.B. Idler, K. Jarvis, E.F. Johnson, L.R. Kleinberg, V. Klinghofer, L.M. Lasko, X. Liu, K.C. Marsh, T.P. McGonigal, J.A. Meulbroek, A.M. Olson, J.P. Palma, L.E. Rodriguez, Y. Shi, J.A. Stavropoulos, A.C. Tsurutani, G.D. Zhu, S.H. Rosenberg, V.L. Giranda, D.J. Frost, ABT-888, an orally active poly(ADP-ribose) polymerase inhibitor that potentiates DNA-damaging agents in preclinical tumor models, Clin. Cancer Res. 13 (2007) 2728–2737.
[13] H. Farmer, N. McCabe, C.J. Lord, A.N. Tutt, D.A. Johnson, T.B. Richardson, M. Santarosa, K.J. Dillon, I. Hickson, C. Knights, N.M. Martin, S.P. Jackson, G.C. Smith, A. Ashworth, Targeting the DNA repair defect in BRCA mutant cells as a therapeutic strategy, Nature 434 (2005) 917–921.
[14] N. Curtin, PARP inhibitors for anticancer therapy, Biochem. Soc. Trans. 42 (2014) 82–88.
[15] P.C. Fong, D.S. Boss, T.A. Yap, A. Tutt, P. Wu, M. Mergui-Roelvink, P. Mortimer, H. Swaisland, A. Lau, M.J. O'Connor, A. Ashworth, J. Carmichael, S.B. Kaye, J.H. Schellens, J.S. de Bono, Inhibition of poly(ADP-ribose) polymerase in tumors from BRCA mutation carriers, N. Engl. J. Med. 361 (2009) 123–134.
[16] M. Anwar, H.M. Aslam, S. Anwar, PARP inhibitors, Hered. Cancer Clin. Pract. 13 (2015) 1–4.
[17] T.D. Penning, G.D. Zhu, J. Gong, V.B. Gandhi, Y. Luo, X. Liu, Y. Shi, V. Klinghofer, E.F. Johnson, D. Frost, C. Donawho, L. Rodriguez, G. Bukofzer, K. Jarvis, J. Bouska, D.J. Osterling, A. Olson, K.C. Marsh, S.H. Rosenberg, V. Giranda, Discovery of the poly(ADP-ribose) polymerase (PARP) inhibitor 2-[(R)-2-methylpyrrolidin-2-yl]-1H-benzimidazole-4-carboxamide (ABT-888) for the treatment of cancer, J. Med. Chem. 52 (2009) 514–523.
[18] K.A. Menear, C. Adcock, R. Boulter, X. Cockcroft, L. Copsey, A. Cranston, K.J. Dillon, J. Drzewiecki, S. Garman, S. Gomez, H. Javaid, F. Kerrigan, C. Knights, A. Lau, V.M.L Jr., I.T.W. Matthews, S. Moore, M.J. O'Connor, G.C.M. Smith, N.M.B. Martin, 4-[3-(4-Cyclopropanecarbonylpiperazine-1-carbonyl)-4-fluorobenzyl]-2H-phthalazin-1-one: a novel bioavailable inhibitor of poly(ADP-ribose) polymerase-1, J. Med. Chem. 51 (2008) 6581–6591.
[19] H.D. Thomas, C.R. Calabrese, M.A. Batey, S. Canan, Z. Hostomsky, S. Kyle, K.A. Maegley, D.R. Newell, D. Skalitzky, L.Z. Wang, S.E. Webber, N.J. Curtin, Preclinical selection of a novel poly(ADP-ribose) polymerase inhibitor for clinical trial, Mol. Cancer Ther. 6 (2007) 945–956.
[20] P. Jones, S. Altamura, J. Boueres, F. Ferrigno, M. Fonsi, C. Giomini, S. Lamartina, E. Monteagudo, J.M. Ontoria, M.V. Orsale, M.C. Palumbi, S. Pesci, G. Roscilli, R. Scarpelli, C. Schultz-Fademrecht, C. Toniatti, M. Rowley, Discovery of 2-{4-[(3S)-piperidin-3-yl]phenyl}-2H-indazole-7-carboxamide (MK-4827): a novel oral poly(ADP-ribose)polymerase (PARP) inhibitor efficacious in BRCA-1 and -2 mutant tumors, J. Med. Chem. 52 (2009) 7170–7185.
[21] G. Papeo, H. Posteri, D. Borghi, A.A. Busel, F. Caprera, E. Casale, M. Ciomei,

A. Cirla, E. Corti, M. D'Anello, M. Fasolini, B. Forte, A. Galvani, A. Isacchi, A. Khvat, M.Y. Krasavin, R. Lupi, P. Orsini, R. Perego, E. Pesenti, D. Pezzetta, S. Rainoldi, F. Riccardi-Sirtori, A. Scolaro, F. Sola, F. Zuccotto, E.R. Felder, D. Donati, A. Montagnoli, Discovery of 2-[1-(4,4-Difluorocyclohexyl)piperidin-4-yl]-6-fluoro-3-oxo-2,3-dihydro-1H-isoindole-4-carboxamide (NMSP118):a potent, orally available, and highly selective PARP-1 inhibitor for cancer therapy, J. Med. Chem. 58 (2015) 6875–6898.

[22] Y. Shen, F.L. Rehman, Y. Feng, J. Boshuizen, I. Bajrami, R. Elliott, B. Wang, C.J. Lord, L.E. Post, A. Ashworth, BMN 673, a novel and highly potent PARP1/2 inhibitor for the treatment of human cancers with DNA repair deficiency, Clin. Cancer Res. 19 (2013) 5003–5015.

[23] B. Wang, D. Chu, Y. Feng, Y.Q. Shen, M. Aoyagi-Scharber, L.E. Post, Discovery and Characterization of (8S,9R)-5-Fluoro-8-(4-fluorophenyl)-9-(1-methyl-1H-1,2,4-triazol-5-yl)-2,7,8,9-tetrahydro-3H-pyrido[4,3,2-de]phthalazin-3-one (BMN 673, Talazoparib), a Novel, Highly Potent, and Orally Efficacious Poly(ADP-ribose) Polymerase-1/2 Inhibitor, as an Anticancer Agent, J. Med. Chem. 59 (2016) 335–357.

[24] A. Ruf, G. de Murcia, G.E. Schulz, Inhibitor and NAD^+ binding to poly(ADP-ribose) polymerase as derived from crystal structures and homology modeling, Biochemistry 37 (1998) 3893–3900.

[25] L. Lehtiö, A.S. Jemth, R. Collins, O. Loseva, A. Johansson, N. Markova, M. Hammarström, A. Flores, L. Holmberg-Schiavone, J. Weigelt, T. Helleday, H. Schüler, T. Karlberg, Structural basis for inhibitor specificity in human poly(ADP-ribose) Polymerase-3, J. Med. Chem. 52 (2009) 3108–3111.

[26] A.W. White, R. Almassy, A.H. Calvert, N.J. Curtin, R.J. Griffin, Z. Hostomsky, K. Maegley, D.R. Newell, S. Srinivasan, B.T. Golding, Resistance-modifying agents. 9.1 synthesis and biological properties of benzimidazole inhibitors of the DNA repair enzyme poly(ADP-ribose) polymerase, J. Med. Chem. 43 (2000) 4084–4097.

[27] J. Yelamos, J. Farres, L. Llacuna, C. Ampurdanes, J. Martin-Caballero, PARP-1 and PARP-2: new players in tumour development, Am. J. Cancer Res. 1 (2011) 328–346.

[28] Y.Q. Wang, P.Y. Wang, Y.T. Wang, G.F. Yang, A. Zhang, Z.H. Miao, An update on poly(ADP-ribose)polymerase-1 (PARP-1) inhibitors: opportunities and challenges in cancer therapy, J. Med. Chem. 59 (2016) 9575–9598.

[29] T. Karlberg, M. Hammarström, P. Schütz, L. Svensson, H. Schüler, Crystal structure of the catalytic domain of human PARP2 in complex with PARP inhibitor ABT-888, Biochemistry 49 (2010) 1056–1058.

[30] Z.X. Zhu, J. Jin, N. Xue, X. Song, X.G. Chen, Development and validation of high-throughput screening assays for poly(ADP-ribose) polymerase-2 inhibitors, Anal. Biochem. 449 (2014) 188–194.

[31] K.S. Putta, P.J. Hergenrother, An enzymatic assay for poly(ADP-ribose) polymerase-1 (PARP-1) via the chemical quantitation of NADt: application to the high-throughput screening of small molecules as potential inhibitors, Anal. Biochem. 326 (2004) 78–86.

[32] W. Minor, M. Cymborowski, Z. Otwinowski, M. Chruszcz, HKL-3000: the integration of data reduction and structure solution – from diffraction images to an initial model in minutes, Acta Crystallogr. Sect. D. Biol. Crystallogr. 62 (2006) 859–866.

[33] P. Emsley, B. Lohkamp, W.G. Scott, K. Cowtan, Features and development of coot, acta crystallographica, section d, Biol. Crystallogr. 66 (2010) 486–501.

[34] G.N. Murshudov, P. Skubak, A.A. Lebedev, N.S. Pannu, R.A. Steiner, R.A. Nicholls, M.D. Winn, F. Long, A.A. Vagin, REFMAC5 for the refinement of macromolecular crystal structures, Acta Crystallographica, Section D, Biol. Crystallogr. 67 (2011) 355–367.